Argonne National Laboratory

REACTOR DEVELOPMENT PROGRAM

PROGRESS REPORT

January 1965

Printed in USA. Price $3.00. Available from the Clearinghouse for Federal Scientific and Technical Information, National Bureau of Standards, U. S. Department of Commerce, Springfield, Virginia

ANL-7003
Reactor Technology
(TID-4500, 37th Ed.)
AEC Research and
Development Report

ARGONNE NATIONAL LABORATORY
9700 South Cass Avenue
Argonne, Illinois 60440

REACTOR DEVELOPMENT PROGRAM PROGRESS REPORT

January 1965

Albert V. Crewe, Laboratory Director
Stephen Lawroski, Associate Laboratory Director

Division	Director
Chemical Engineering	R. C. Vogel
Idaho	M. Novick
Metallurgy	F. G. Foote
Reactor Engineering	L. J. Koch
Reactor Physics	R. Avery
Remote Control	R. C. Goertz

Report Coordinated by
R. M. Adams and A. Glassner

Issued February 18, 1965

Operated by The University of Chicago
under
Contract W-31-109-eng-38
with the
U. S. Atomic Energy Commission

FOREWORD

The Reactor Development Program Progress Report, issued monthly, is intended to be a means of reporting those items of significant technical progress which have occurred in both the specific reactor projects and the general engineering research and development programs. The report is organized in a way which, it is hoped, gives the clearest, most logical over-all view of progress. The budget classification is followed only in broad outline, and no attempt is made to report separately on each sub-activity number. Further, since the intent is to report only items of significant progress, not all activities are reported each month. In order to issue this report as soon as possible after the end of the month editorial work must necessarily be limited. Also, since this is an informal progress report, the results and data presented should be understood to be preliminary and subject to change unless otherwise stated.

The issuance of these reports is not intended to constitute publication in any sense of the word. Final results either will be submitted for publication in regular professional journals or will be published in the form of ANL topical reports.

The last six reports issued in this series are:

July 1964	ANL-6923
August 1964	ANL-6936
September 1964	ANL-6944
October 1964	ANL-6965
November 1964	ANL-6977
December 1964	ANL-6997

TABLE OF CONTENTS

		Page
I.	Liquid-metal-cooled Reactors	1
	A. General Fast Reactor Physics	1
	1. ZPR-III	1
	2. ZPR-VI	2
	3. ZPPR	7
	4. ZPR-IX	9
	5. Argonne Fast Source Reactor Experiments	10
	B. Fast Reactor Systems and Concepts	13
	1. 1000-MWe Metal-fueled Fast Breeder Reactor Study	13
	C. General Fast Reactor Fuel Development	14
	1. Development of Jacket Materials	14
	2. Corrosion Inhibition in Sodium	16
	3. Irradiation of Experimental and Prototype Fuels	16
	4. Elements for Alpha and Breeding-gain Measurement	17
	5. Zero-power Reactor Fuels	18
	D. General Fast Reactor Fuel Reprocessing Development	20
	1. Advanced Processes	20
	2. Materials and Equipment Evaluation	20
	3. Eddy Current Induction Probe	21
	4. Decladding Studies for TV-20 Cladding	22
	E. Liquid Sodium Coolant Chemistry	23
	F. EBR-II	25
	1. Removal of Oscillator Rod and Thimble	25
	2. Inadvertent Raising of the Safety Rods	26
	3. Plant Maintenance and Modification	27
	4. Fuel Cycle Facility	28
	G. FARET	32
	1. General	32
	2. Neutron Shield	33

TABLE OF CONTENTS

		Page
	3. Safety Analysis	34
	4. Shielded Windows	34
	5. Control Rod Drive Seal Tests	34
	6. Fuel Slip-fit Experiment	37
	7. Fuel Assembly Sodium Flow Test Loop	37
	8. Core Support Analysis	37
II.	General Reactor Technology	38
	A. Experimental Reactor and Nuclear Physics	38
	1. Cherenkov Counting of Aqueous Solutions	38
	2. Fast-neutron Hodoscope	39
	B. Theoretical Reactor Physics	40
	1. ZPR-VII Data Analysis	40
	C. High-temperature Materials	41
	1. Preparation of Uranium Monosulfide	41
	2. Properties of (Th-U-Pu) Phosphides	41
	3. Mechanical Properties of Uranium Compounds	43
	4. Thermal Stability	44
	5. Anelasticity of Some Uranium Compounds	44
	6. Corrosion by Liquid Metals	44
	D. Other Reactor Fuels and Materials Development	48
	1. Nondestructive Testing	48
	E. Engineering Development	48
	1. Development of Manipulators for Handling Radioactive Materials	48
	2. Two-phase Flow Studies	50
	3. Boiling Liquid Metal Technology	50
	4. General Heat Transfer	52
	5. ANL-AMU Program	53

TABLE OF CONTENTS

	Page
F. Chemical Separations	57
1. Fluoride Volatility Processes	57
2. General Chemistry and Chemical Engineering	61
G. Plutonium Recycle Reactors	62
1. Physics Calculations	62
2. Fuel Development and Fabrication	64
3. EBWR Facility	65
III. Advanced Systems Research and Development	68
A. Argonne Advanced Research Reactor	68
1. Design of the Outer Radial Reflector: Theory	68
2. Heat Transfer	70
3. Transient Analysis	72
4. Instrumentation Control Design	73
5. Critical Experiment	74
B. Regenerative Fuel Cells	74
1. Bimetallic Cells	74
IV. Nuclear Safety	76
A. Chemical Reactions	76
1. Metal-Water Reactions	76
B. Reactor Kinetics	77
1. Fast Reactor Safety	77
2. TREAT Operations	79
V. Publications	81

I. LIQUID-METAL-COOLED REACTORS

A. General Fast Reactor Physics

1. ZPR-III

a. FARET Mockup. Construction of ZPR-III Assembly 46, for the mockup studies of the FARET first core loading, was begun. The FARET system is envisioned as a 2-ft-long by 14-in.-diameter core with steel radial and axial reflectors. The fuel will consist of either oxides or carbides of plutonium and uranium, or a mixture of the two. Experiments will be concerned with these different possible fuel loadings.

The first phase of the experiments, designated Assembly 46A, will be a study of a carbide-fueled core, mocking up a possible FARET core composition of 36 v/o (PuU)C, 44 v/o sodium, and 20 v/o steel. In this mockup, the fuel will be simulated with plates of plutonium, uranium, and graphite. Preliminary calculations indicate an expected critical loading of 67 liters, using a U-to-Pu ratio of 6 and with the uranium enriched to about 40% with U^{235}. A core-drawer loading approximating these compositions will be used for the 46A experiments.

The reflectors for the core in the Assembly 46 experiments simulate those expected for FARET. Axially, the reflector contains about 55 v/o steel and 38 v/o sodium, representing the axial ends of FARET core subassembly with the fuel replaced by steel. The FARET radial reflector subassemblies, containing 82 v/o steel and 18 v/o sodium, are mocked up in Assembly 46 with various combinations of steels, sodium, and aluminum. A possible sodium plenum around the steel reflector in FARET is also represented. Construction of these various reflector regions in the ZPR-III machine has been completed and core-loading operations have been initiated.

b. Preliminary Results on Assembly 45A. Preliminary analyses have been completed for the experiments performed with Doppler Assembly 45A.

The central fission ratios were measured, both with heavy-walled Kirn counters with sealed counting gas and with thin-walled gas flow counters. The Kirn counters were used because gas-flow foils are not available for all the isotopes of interest. The results are listed in Table I.

The central reactivity worth of plutonium was measured using two 1/8 x 2 x 2-in. standard fuel plates, each one loaded across the front fourth of a drawer. The two drawers were nonopposing to reduce heterogeneity effects. The depleted uranium worth was measured by removing one-third of the depleted uranium from the first 3 in. of each drawer for

the central nine drawers of the central zone. The central worth of sodium was measured by removing all of the first 4 in. of sodium from a five-drawer cell in the central zone. The full-length axial worth of sodium (core and axial blanket) was measured by removing all of the sodium from a four-drawer cell of the central zone and axial blanket. The results are given in Table II, in which the reported worths are corrected for the stainless steel canning materials.

Table I. Central Fission Ratios - Assembly 45A

	$\sigma_f(i)/\sigma_f(U^{235})$	
i	Thin-walled Counters	Thick-walled Counters
U^{238}	0.0279 ± 2%	
U^{236}		0.0627 ± 2%
U^{234}		0.182 ± 2%
Pu^{240}		0.218 ± 5%
Pu^{239}		1.047 ± 3%
U^{233}	1.44 ± 2%	

Table II. Central Reactivity Measurements - Assembly 45A

Sample	Mass (kg)	Worth (Ih ± 0.5)	Reactivity Coefficient with Respect to Void (Ih/kg)
Pu fuel plates	0.139	+24.4	+176 ± 4
Depleted uranium	4.03	-30.6	-7.6 ± 0.1
Na (central)	1.222	-5.8	-4.7 ± 0.4
Na (axial)	8.06	+19.1	+2.37 ± 0.06

The axial reaction rate traverses were performed in the usual manner of driving a 2-in.-long counter to specific positions in the reactor and measuring the counting rate at each location. The data represent count rates averaged over the 2-in. length of the counter. The results are given in Table III.

2. ZPR-VI

Axial and radial fission ratio traverses were made in Assembly No. 3 with U^{235} and U^{238} foils. The measurements were made with the core in its normal configuration and with the sodium voided from different parts of the core. In addition, the fine-structure distribution of the fission rate across one drawer near the center of the core was also measured.

Table III. Normalized Axial Reaction Rate Traverses - Assembly 45A

Distance from Reactor Midplane, cm	Pu^{239}	U^{238}	U^{238}/Pu^{239}
+62.2	0.174 ± 1.2%	0.044 ± 3.6%	0.251 ± 3.8%
+54.6	0.275 ± 1.0%	0.106 ± 2.4%	0.385 ± 2.6%
+49.5	0.358 ± 1.0%	0.180 ± 1.8%	0.502 ± 2.0%
+47.0	0.398 ± 1.0%	0.299 ± 1.6%	0.575 ± 1.9%
+45.8	Axial blanket/core interface		
+44.4	0.452 ± 0.9%	0.326 ± 1.4%	0.722 ± 1.6%
+41.9	0.488 ± 0.9%	0.409 ± 1.5%	0.838 ± 1.7%
+39.4	0.542 ± 0.9%	0.486 ± 1.4%	0.898 ± 1.6%
+34.3	0.640 ± 0.8%	0.610 ± 1.3%	0.953 ± 1.5%
+29.2	0.735 ± 0.8%	0.727 ± 1.2%	0.988 ± 1.4%
+24.1	0.828 ± 0.8%	0.825 ± 1.1%	0.996 ± 1.4%
+19.0	0.903 ± 0.8%	0.893 ± 1.1%	0.989 ± 1.3%
+14.0	0.942 ± 0.8%	0.942 ± 1.0%	1.000 ± 1.3%
+8.9	0.981 ± 0.8%	1.006 ± 1.0%	1.025 ± 1.3%
+3.8	1.000 ± 0.8%	1.009 ± 1.0%	1.008 ± 1.3%
+1.3	0.994 ± 0.8%	0.990 ± 1.0%	0.995 ± 1.3%
0	Reactor midplane		
-1.3	1.008 ± 0.8%	0.996 ± 1.0%	0.989 ± 1.3%
-3.8	0.987 ± 0.8%	1.000 ± 1.0%	1.014 ± 1.3%
-6.3	0.981 ± 0.8%	0.991 ± 1.0%	1.010 ± 1.3%
-11.4	0.984 ± 0.8%	0.941 ± 1.0%	0.956 ± 1.3%
-16.5	0.924 ± 0.8%	0.921 ± 1.0%	0.997 ± 1.3%
-21.6	0.856 ± 0.8%	0.844 ± 1.1%	0.987 ± 1.3%
-26.7	0.774 ± 0.8%	0.765 ± 1.1%	0.989 ± 1.4%

The measurements were made for the following configurations:

a. the original core loading;

b. the core with a sodium-voided central region having a nominal radius of 25 cm;

c. the core with the sodium voided from a sector extending from the core center to its radial boundary and comprising one-eighth of the total core.

The arrangement of the materials in a core drawer is shown in Figure 1. For the axial and radial traverses, the foils were placed between the U^{238} and graphite plates in the center of the drawer. For the radial traverses, the foils were placed at the front end of the drawer in different radial locations. For the axial traverses, the foils were placed in the center drawer (location 2323) at different distances from the

interface of the halves. For the measurement of the fine distribution through a drawer, the foils were placed between each two adjoining plates of the core materials at the front end of a drawer near the center of the assembly.

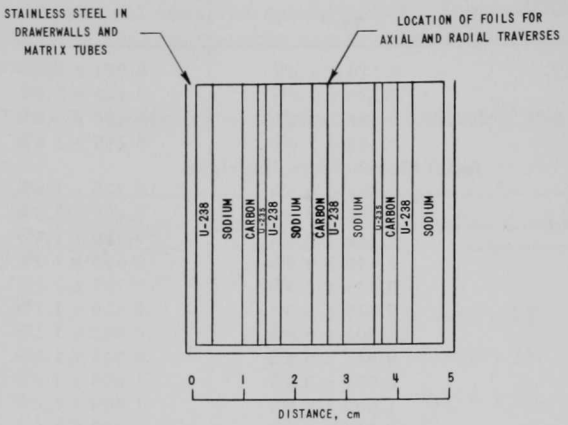

Figure 1. Material Arrangement in Core Drawer (front view)

Figures 2 through 5 show the measured variations of the U^{238}/U^{235} fission ratio. All values were normalized to unity at the core center for the axial and radial traverses, and at the center of the drawer (between the U^{238} and carbon plates) for the fine distribution measurements.

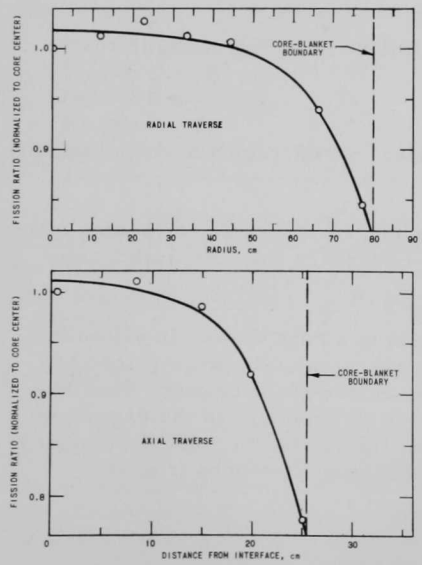

Figure 2

Fission Ratios for the Original Core Loading (normalized to unity at the core center)

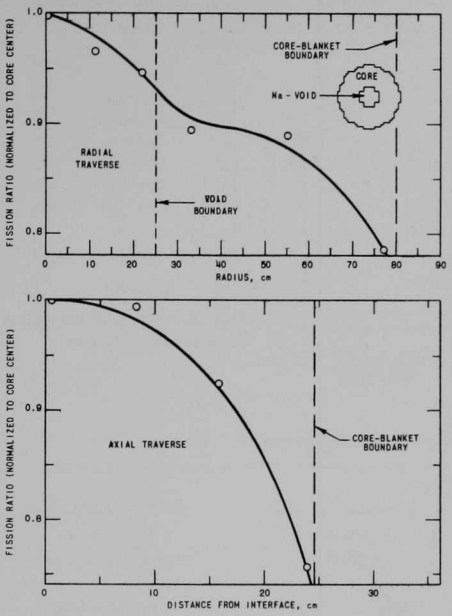

Figure 3
Fission Ratios with the
25-in.-radius Central Void

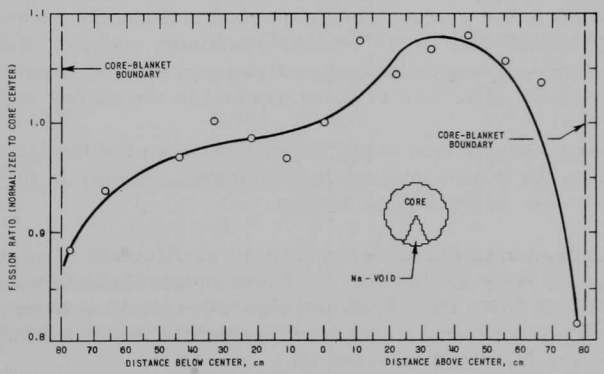

Figure 4. Radial Fission Traverse with the Voided Sector

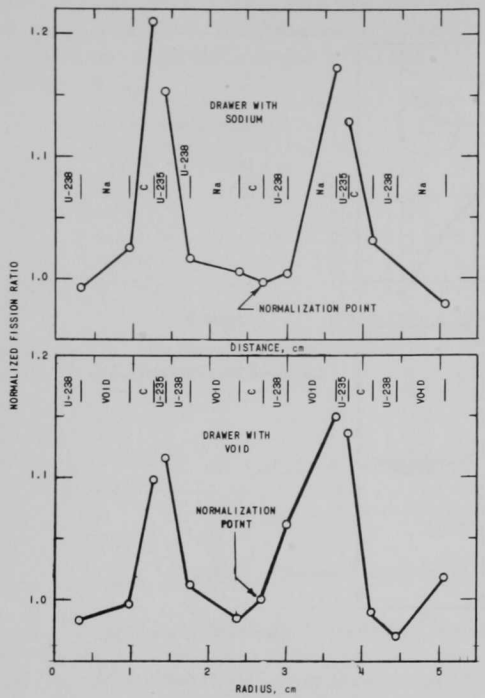

Figure 5

Fine Distribution of the Fission Ratio through a Drawer

Figures 3 and 4 show that the fission ratio in the voided regions is about 10% higher than in the regions containing sodium. They also show that near the core boundary the transition from the soft blanket spectrum to the harder core spectrum is more gradual in the voided regions.

Figure 5 shows that the difference between the fission ratio near the fuel and in the diluent materials is somewhat higher in the sodium-filled drawer than in the voided drawer.

Measurements of central reactivity coefficients of various materials were also made in Assembly No. 3. These measurements were made at the center of the core, once when the central region had been voided of sodium and again when the central region had the normal amount of sodium. The results are tabulated in Table IV.

A number of fission ratios of other isotopes were measured at the center of the core of Assembly No. 3 with a pair of absolute gas-flow fission counters. Measurements were also made with and without sodium in the central region of the core. The results are shown in Table V.

Table IV. Central Reactivity Coefficients from Assembly No. 3

Material	Nominal Size (in.)	Total Weight (g)	Central Region with Sodium		Central Region with Void	
			Ih	Ih/kg	Ih	Ih/kg
U^{235}	2 x 2 x 1/4	292.9	+21.3 ± 0.5	+72.7 ± 1.7	+18.9 ± 0.5	+64.5 ± 1.7
U^{235}	2 x 2 x 1/8	146.3	+10.3 ± 0.5	+70.4 ± 3.4	-	-
Pu	2 x 2 x 1/4	123.4	+14.8 ± 0.5	+119.9 ± 4.0	+12.9 ± 0.5	+104.5 ± 4.0
U^{233}	2 x 2 x 1/4	110.9	+16.1 ± 0.5	+145.2 ± 4.5	+13.2 ± 0.5	+119.0 ± 4.5
U^{233}	2 x 2 x 1/4	147.6	+20.3 ± 0.5	+137.5 ± 3.4	-	-
U^{238}	2 x 2 x 1	1154	-4.75 ± 0.030	-4.12 ± 0.03	-3.951 ± 0.03	-3.42 ± 0.03
Al	2 x 2 x 1	166.9	-0.071 ± 0.030	-0.43 ± 0.18	-0.246 ± 0.030	-1.47 ± 0.18
Al_2O_3	2 x 2 x 1	237.9	+0.395 ± 0.030	+1.66 ± 0.13	+0.104 ± 0.030	+0.44 ± 0.13
SS	2 x 2 x 1	500	-1.120 ± 0.030	-2.24 ± 0.06	-1.123 ± 0.030	-2.24 ± 0.06
Fe	2 x 2 x 1	488	-1.106 ± 0.030	-2.26 ± 0.06	-1.033 ± 0.030	-2.12 ± 0.06
Fe_2O_3	2 x 2 x 1	299	+0.041 ± 0.030	+0.14 ± 0.10	-0.237 ± 0.030	-0.79 ± 0.1
C	2 x 2 x 1	103	+1.073 ± 0.030	+10.4 ± 0.3	+0.808 ± 0.030	+7.84 ± 0.3
Critical Mass:			853 kg U^{235}		875 kg U^{235}	

Table V. Fission Ratios in Assembly No. 3

Isotopes Used in Ratio Measurements	Fission Ratios	
	Sodium-filled Region	Void Region
U^{233}/U^{235}	1.545 ± 0.020	1.550 ± 0.020
U^{234}/U^{235}	0.233 ± 0.005	0.251 ± 0.005
U^{236}/U^{235}	0.075 ± 0.005	0.076 ± 0.005
U^{238}/U^{235}	0.0346 ± 0.0005	0.0382 ± 0.0005
Np^{237}/U^{235}	0.258 ± 0.006	0.287 ± 0.006
Pu^{239}/U^{235}	1.044 ± 0.020	1.063 ± 0.020
Pu^{240}/U^{235}	0.244 ± 0.006	0.259 ± 0.006

3. ZPPR

The architect engineering firm of Mason-Hanger, Silas-Mason Co., Inc., is now in the process of preparing the Title I report. The outline specifications for the ANL-furnished equipment were completed for Title I.

The technical specifications for the bed and tables have been completed and are ready to go out for bids. Figure 6 is a drawing showing the reactor perspective.

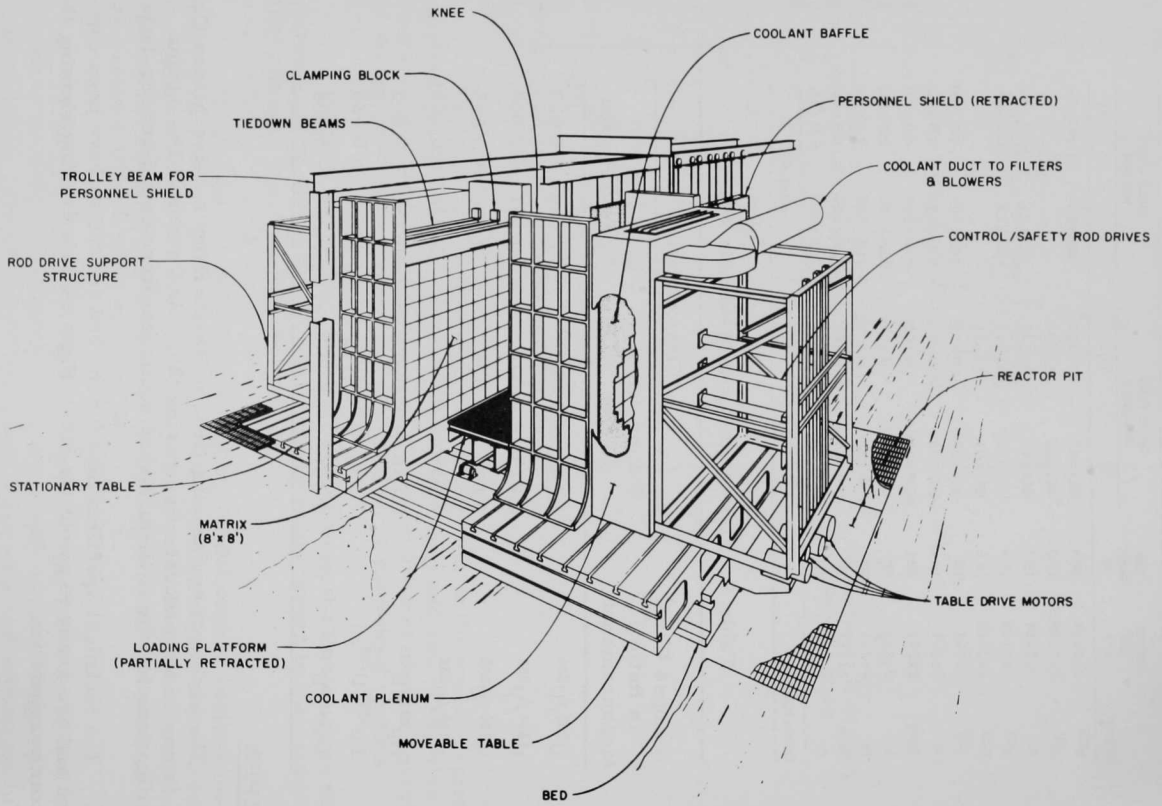

Figure 6. Perspective of Zero Power Plutonium Reactor

a. Reactor Cooling. Additional tests (see Progress Report for December 1964, ANL-6997, pp. 2-3) were made, using a 9-tube mockup of the core. The results agreed with those of the tests with single tubes.

The drawers used in the tests were filled with perforated aluminum mockup pieces so that the drawers were light in comparison to any that might have depleted uranium or fuel. It was observed that when the flow was high enough to cause a pressure drop in excess of 12 in. H_2O across the 4-ft-long tubes, the last drawer tended to be moved out of the tubes. Drawers with heavier loadings would require higher pressure differentials to cause movement.

In the design and specification of the tubes, adequate allowance will be made for coolant channels to keep pressure drops below that which would cause movement of drawers by the coolant flow.

b. Reactor Fuel Design. Some preliminary design work has been started to formulate the fuel-jacket requirements for ZPPR fuel. Since the fuel will be used in a loading machine, adaptability to machine loading is one of the major requisites for this design. Other criteria are being developed to include in the design.

4. ZPR-IX

A digital method for calibrating control rods[1] is being investigated for use with the ZPR-IX assembly. A system is being developed for on-line reactor operation so as to provide direct computer input.

A multiscaler, operating at count rates of 5,000-10,000 counts per 0.5 sec, is used to prepare input tapes to the DDP-24 computer. The computer output is fed to an on-line graph plotter which provides a curve of the control rod worth versus position. Positions were established by noting the time the rod motion is started and stopped, and by assuming the motion occurs at uniform speed. Good agreement was found between the results of this method and the calibrations obtained by period measurements. However, the reactivity traces shown on the output curves had random fluctuations, amounting to 5 to 10% of the indicated values.

Two methods of data manipulation were tried for smoothing out these fluctuations. One method uses a truncated Fourier analysis;[2] another makes use of the fact that the flux must monotonically decrease during rod

[1] Cohn, C. E., and Kaganove, J. J., Digital Method for Control Rod Calibrations, Trans. Am. Nucl. Soc. 5, 388 (Nov. 1962).

[2] Lanczos, C., Evaluation of Noisy Data, J. Soc. for Industrial and Appl. Math. B1, 76 (1964).

withdrawal and thereby wipe out all upward fluctuations. Neither method gave a useful degree of smoothing and both tended to introduce bias. It is planned to improve the measurements by use of a higher-speed counter or a voltage-to-frequency converter in conjunction with an electrometer.

The digital method was also used to measure gap worth. With the reactor at critical, the halves were separated at a velocity of 1.3 cm/min and the flux level measured continuously. The results of this test indicated, however, that the gap worth was only one-tenth of that found for Assembly No. 4. Since the gap worth values were expected to be relatively close, it appears that these results were influenced by the location of the counter. The counter was placed near the bottom of the matrix against the interface and apparently was not effectively shielded from the core flux as the gap was increased. It therefore indicated a smaller change in reactivity with increasing gap. It is planned to repeat the experiment with the counter placed in a more fortuitous position.

5. Argonne Fast Source Reactor Experiments

a. Pulsed Neutron Experiments. The pulsed neutron experiments accomplished in AFSR during December have been analyzed. Figure 7 is a plot of the values obtained for the exponential decay constant (α) versus reactivity. Extrapolation yields a value of $(3.50 \pm 0.05) \times 10^5$ for α at delayed critical, in satisfactory agreement with the value $(3.65 \pm 0.10) \times 10^5$ obtained by the Rossi-alpha method in 1960. Since the AFSR core was recanned in 1961, with 15-mil stainless steel replacing 5 mils of nickel and the change yielded a slightly more dilute core with about 0.5% greater critical mass, this may account for the small discrepancy between the two values.

Note that α extrapolates to 0 about 370 Ih above delayed critical, whereas the value calculated from the inhour equation for prompt critical is 300 ± 2 Ih. This anomaly has been noted before in Rossi-alpha results reported previously;[3] however, the results in this case have a much smaller uncertainty due to the improved statistics obtained with the pulsed neutron source. The same anomaly was reported recently by W. J. Paterson and J. W. Weale of Aldermaston. Their work with VERA showed a similar discrepancy in uranium systems and relatively much larger discrepancies in plutonium systems. Study is under way to explain this phenomenon, since it reflects on our ability to calculate the absolute delayed-neutron fraction or to measure reactivity.

b. Modifications to Pulsed Neutron Source. The manufacturer has supplied an improved accelerating tube for the pulsed neutron source. Installation of the new unit was completed and the machine was checked out

[3] Brunson, G. S., et al., A Survey of Prompt Neutron Lifetimes in Fast Critical Systems, ANL-6681 (Aug 1963).

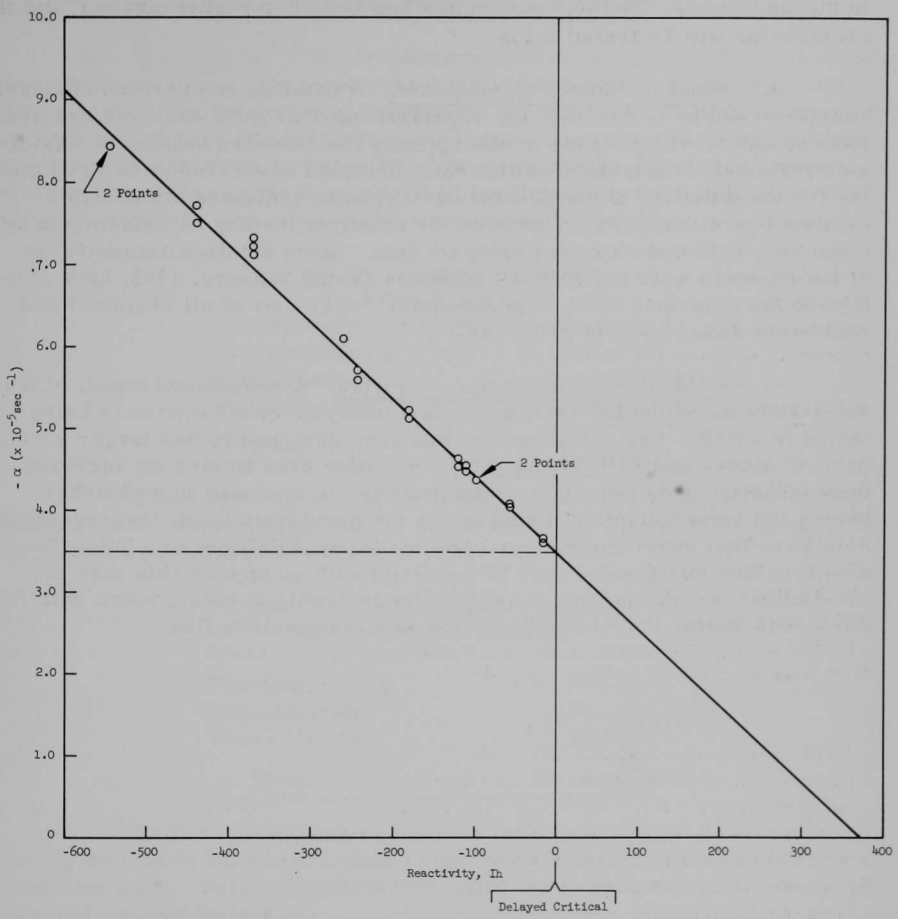

Figure 7. Neutron Pulse Decay Constant (α) as a Function of Reactivity in AFSR

by a manufacturer's representative. The equipment was operable but did not attain the expected beam current due to an apparent voltage breakdown in the ion source. The ion source has now been thoroughly cleaned, and the accelerator will be tested again.

c. Fission Counter Comparison. A detailed comparison of fission counters used by APDA with the regularly used ZPR-III counters has been carried out for the purpose of determining the effective amount of fissionable material. Analysis of initial data, obtained several months ago following the construction of the counters at Argonne, indicated the possible existence of discrepancies between the effective loading as determined by count rate data and chemical analysis data. More detailed comparisons of the counters with the ZPR-III counters during January, 1965, have confirmed the existence of the discrepancies. A review of all chemical and count rate data is now in progress.

d. Solid-state Neutron Spectrometry. A redesigned model of the solid-state detector-Li^6 "sandwich" fast-neutron spectrometer is being tested in AFSR. The spectrometer has been designed to use larger surface-barrier diodes and Li^6-bearing films of larger area to give an increase in sensitivity. The redesigned spectrometer is enclosed in a chamber having the same outside dimensions as the previously used, less-sensitive model, so that experiments may continue in the AFSR grazing hole. Indications are that this end may be achieved with no appreciable loss of resolution. An increase in sensitivity is desirable to obtain more data from the diodes during their useful lifetime in a fast neutron flux.

B. Fast Reactor Systems and Concepts

1. 1000-MWe Metal-fueled Fast Breeder Reactor Study

a. Fuel Cycle. The preliminary capital costs presented previously (see Progress Report for December 1964, ANL-6997, p. 5) covered only the direct costs. The total capital investment for a fuel-cycle plant designed for the capacity of core and blankets discharged from and needed for the reference reactor are given in Table VI. The construction overhead, startup costs, and working capital were added to the figures presented in ANL-6997, and a re-estimate was made of the waste-handling facility.

Table VI. Capital Costs for Fuel Cycle Facility

Pyroprocessing	$ 5,973,000
Refabrication	9,278,000
Waste Facility	1,901,000
Total	$17,152,000

The annual operating costs for this plant, including direct and indirect labor, operating materials and utilities, and general overhead and administrative expense are given in Table VII.

Table VII. Annual Operating Costs for Fuel Cycle Facility

Pyroprocessing	$ 756,000
Refabrication	3,793,000
Waste Facility	132,000
Total	$4,681,000

An initial estimate of the size influence of such a fuel cycle facility was made based on a plant capacity 2.5 times that needed for the reference plant. This indicated a 30% unit cost reduction for the combined core and blanket fuels.

Supplemental to the overall fuel-cycle cost studies, is a study of the refabrication covering the influence of variables such as fuel designs, materials, element size, and capacity. A computer program having about 200 variables has been set up. The equations characterize the fabrication cost of fuel rods. Figure 8 illustrates one of the study results using a fuel element design where the core and axial blanket sections are contained in the same cladding tube. The major direct costs involved in refabrication study are used.

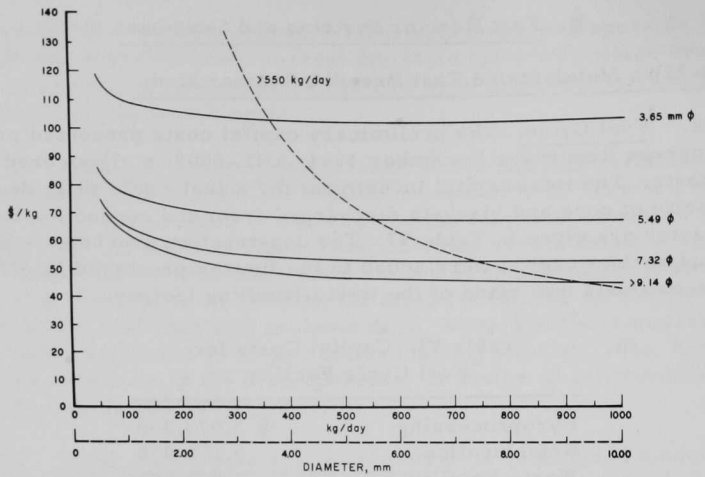

Figure 8. Preliminary Computations of Refabrication Costs in $/kg vs. Plant Throughput and Fuel Diameter

C. General Fast Reactor Fuel Development

1. Development of Jacket Materials

a. Vanadium Alloys

(i) Commercial Extrusion. Following the development by the Argonne Metallurgy Division of methods of fabricating V-20 w/o Ti (TV-20) and the selection of this alloy as a likely material for the jacketing of fast reactor fuels, industry was encouraged to participate in its production and fabrication development. Commerical extrusion of 15.2-cm (6-in.) diameter ingots of TV-20 produced by Union Carbide Corporation (Stellite Division) has now been demonstrated by the Canton Drop Forge Company, Canton, Ohio.

Two ingots, contained in a single mild-steel can, were extruded to bar stock at 1100°C and an approximate 7:1 reduction ratio. The billet extruded satisfactorily despite the leakage of salt through a defective closure weld into the can during salt-bath preheating. Declad extruded bar stock received at ANL is now being analyzed to determine if any reaction occurred between the salt and the TV-20.

(ii) Corrosion by Sodium. A second series of recrystallized V-20 w/o Ti tensile samples has been exposed to flowing sodium (0.15 cm/sec) for seven days at 650°C. Three of the samples were allowed to undergo creep (average strain was 1.5%) during the test, and two samples were unstressed. The average weight loss for both the stressed and unstressed samples was 1.8 mg/cm^2. There was no effect of stress on weight loss. Metallographic examination of these samples is now in progress.

The corrosion product has been identified by X-ray diffraction techniques as $VO_{0.9}$. Presence of titanium in the oxide is suspected

because of the fogging of the X-ray film, which could have been caused by fluorescence of titanium. An attempt to confirm the presence of titanium by chemical analysis of the corrosion product will be made.

Malfunctioning of the plugging meter prevented any indication of the oxygen level during the experimental run. Samples have been taken for the determination of the oxygen concentration by chemical methods.

Because of the necessity for accurate determination of oxygen concentrations in our liquid sodium systems, work is in progress to modify and refine our equipment and techniques for the determination of low levels of oxygen (less than 100 ppm) in sodium. Definite progress has been made toward the achievement of accurate and reproducible results in a routine manner.

b. Development of Refractory-Metal Alloys for Service in Oxygen-contaminated Sodium. A small recirculating system for corrosion testing in 650°C sodium has been completed and is being checked. A flow of about 70 cc/min of sodium is circulated through a lower-temperature leg and filter to establish a known oxygen content in the test autoclave. Difficulty is being experienced with the small diaphragm pump.

c. Compatibility

(i) Interaction of (U, Pu)C with Potential Cladding Materials. Compatibility between fuel and cladding is a prime consideration in the selection of an optimum cladding material for (U, Pu)C fast reactor fuels. Therefore, a systematic study of potential claddings in the temperature range from 650 to 1100°C has been started. The study will cover pure metals as well as alloys based on iron, nickel, and a number of refractory metals.

Diffusion couples made from the first batch of $(U_{0.8}Pu_{0.2})C$ pellets have been annealed according to the schedule given in Table VIII and are being evaluated metallographically and by microhardness measurements. Additional $(U_{0.8}Pu_{0.2})C$ pellets now on hand will be made into diffusion couples to be annealed at times and temperatures consistent with evaluations of the above 32 couples.

Table VIII. Completed Diffusion-Couple Annealings

	7 Days		17 Days		42 Days	
Cladding Materials	950°C	1100°C	950°C	1100°C	950°C	1100°C
Hastelloy-X	X	X	X	X	X	X
Type 304 SS	X	X	X	X	X	X
Vanadium	X	X	X	X	X	X
V-20 w/o Ti	X	X	X	X	X	X
Chromium	X	X				
Niobium	X	X				
Molybdenum		X				
Tantalum		X				
Ta-10 w/o W		X				
Tungsten		X				

2. Corrosion Inhibition in Sodium

An isothermal-sodium-solution flow loop has been designed for the study of corrosion of solid structural materials, such as vanadium, zirconium, and titanium alloys, in liquid sodium containing dissolved getter elements at temperatures up to about 650°C. Minor modifications would permit operation to the boiling point. Flow is considered essential to such a study since concentrations of impurities of interest, such as oxygen, are expected to be low, resulting in serious local depletion of impurity in the absence of flow.

Depletion of oxygen impurity at sample surfaces due to the stationary liquid boundary layer (in spite of flow) is thought to be unlikely on the basis of estimates of diffusion and corrosion rates. For an estimated diffusion coefficient of 10^{-4} cm^2/sec and an effective boundary layer thickness of 10 μ, the limit of the flux rate at a bulk concentration of 1 ppm oxygen is 10 to 100 times the oxidation rates expected of the solid materials. Under these conditions the requirement is to deliver sodium containing the desired concentration of solute to the general vicinity of the sample at a rate sufficient to prevent local depletion.

The loop design provides for sodium pumping at a rate of 1.5 liter/min in 1-in. standard (2.5-cm-ID) pipe, yielding a flow velocity of 4.5 cm/sec in an unrestricted section of the pipe. The total volume of sodium employed will be about 850 cc. The pump will consist of two, series, in-line, ball check valves operated at test temperature with argon-filled void spaces above the sodium on either side. The moderate argon pressures (≈17 psia or 1.2 kg/cm^2) are to be cycled to effect sodium pumping.

The loop is to be constructed of nickel, based on experience in static tests. Some dissolution of the nickel by test sodium is expected and will be tolerated in the initial work. Static corrosion test exposure of commercially pure nickel to sodium containing 1 w/o calcium getter for 5.5 days at 680°C resulted in small average weight changes of the order of 0.1 mg/cm^2 and no serious effect on appearance. Resistance of nickel to air oxidation has been observed to be satisfactory in this temperature range. Although mechanical properties appear poor at such temperatures, the requirement for strength is moderate in this application.

Loop components and instruments are being procured.

3. Irradiation of Experimental and Prototype Fuels

a. Full-length EBR-II Fuel Elements of Refractory Alloy-jacketed Uranium-Plutonium-Fissium Alloy. Capsules containing full-length [45 cm (18 in.)] EBR-II fuel elements of refractory alloy-jacketed U-Pu-Fs alloys are being irradiated in the MTR. The temperature in the capsules is controlled by varying the composition of a helium-nitrogen mixture in an annulus surrounding the fuel specimens.

Capsule ANL-55-6 contained three identical fuel elements. The fuel was U-20 w/o Pu-10 w/o Fs alloy jacketed in stress-relieved Nb-1 w/o Zr alloy tubing, 3.96 mm in ID and of 0.23-mm wall thickness. This capsule was put into the MTR on April 15, 1963, and removed on July 20, 1964, after 2.4 percent burnup of heavy-metal atoms. Jacket temperatures were about 505°C at the hottest sections. Temperature data for this irradiation experiment had given no indication of any failure.

When the capsule was returned to the Illinois site it was neutron radiographed. One fuel element showed evidence of a fairly long split in the jacket on the lower half. There was only slight evidence of fuel swelling on this element. The other two elements appeared to be intact. In all three elements the fuel pins were displaced about 20 mm off of the bottom plug within the jackets.

The capsule was taken apart in the Alpha-Gamma Hot Cell (in Building 212) and the fuel elements were removed without difficulty. The crack noted on the neutron radiograph was found to extend from about 25 mm above the lower end of the element for a total length of 115 mm. The crack extended into the fuel for a short distance and had the appearance of a rip or a tear. The spacer discs appear to have had only a slight restraining effect on the splitting action. The other two fuel elements seemed to be in good condition. Further examination is under way.

b. Postirradiation Examination of EBR-I Mark-IV Plutonium Fuel Rods. Eleven rods representing a complete radial section from the center to the edge of the EBR-I Mark-IV core were delivered to the Alpha-Gamma Hot Cell for examination. The maximum fuel burnup is 0.07 a/o. The Pu-1.25 w/o Al alloy fuel rods were NaK-bonded in Zircaloy-2 tubes. Diameter measurements made at 2.5 cm (one-inch) intervals along the length of each jacketed rod disclosed no significant dimensional changes. After decanning, the dimensions of the fuel slugs will be compared with preirradiation values for more definitive information concerning the fuel behavior. Postirradiation examination also will include density measurements of the bare fuel and metallographic examination of representative samples.

4. Elements for Alpha and Breeding-gain Measurement

Seven special EBR-II core rods containing 33 isotope sample capsules, four axial blanket rods containing 12 capsules, and five radial blanket rods containing 20 capsules, were assembled into three special EBR-II fuel rods and five blanket elements meeting EBR-II standards. The elements are identified in Table IX.

Table IX. Identity, Position, and Content of Breeding Gain Elements

Identity No.	Reactor Position	Contents
C220X	Core, Row 1	86 standard fuel rods (5835.19 g U-Fs Alloy 5543.43 gU, 2668.10 g U^{235})
		5 rods, each containing 5 capsules
		32 standard axial blanket rods
		4 upper blanket rods each containing 3 capsules
C221X	Core, Row 3	90 standard fuel rods (6075.09 g U-Fs Alloy 5771.33 g U, 2777.75 g U^{235})
		1 rod containing 4 capsules
		36 standard axial blanket rods
C222X	Core, Row 5	Loaded as C221X (6047.96 g U-Fs Alloy, 5745.56 g U, 2765.33 g U^{235})
A776X	Inner Radial Blanket, Row 7	18 standard radial blanket rods 1 rod containing 4 capsules
U1548X	Outer Radial Blanket, Row 9	Loaded as A776X
U1549X	Outer Radial Blanket, Row 11	Loaded as A776X
U1550X	Outer Radial Blanket, Row 13	Loaded as A776X
U1551X	Outer Radial Blanket, Row 15	Loaded as A776X

5. Zero-power Reactor Fuels

a. Fabrication of U^{233} Reactivity Coefficient Specimens for ZPR-VI. Six 42 x 45 x 4.5-mm plates were fabricated from U^{233} for reactivity measurements in ZPR-VI. A quantity of 1288 grams U^{233} containing 42 ppm of U^{232} was separated on November 19 and reduced to metal at ORNL. It was received at ANL on December 10. At this time the largest piece weighing about 800 grams produced a reading of 1 r/hr gamma at 50 mm through a 0.7 mm rubber glove. On December 21, just prior to casting, the same piece produced a reading of 6.5 r/hr gamma at 50 mm.

Because of the rapid build-up of gamma radioactivity, it was desirable to fabricate this material as quickly as possible. A fabrication plan was adopted that by rotating personnel required no person to spend more than one-half hour with his hands closer to the material than 30 cm. Wrist badges were worn and in some cases light lead shielding was used. The procedure was rehearsed by fabricating depleted uranium specimens. A stop watch log was kept of each individual's exposure.

Casting into precision graphite molds was selected as the method for fabricating the required core plates that would minimize exposure of personnel to radiation. The plates were double jacketed in 0.38-mm-thick Type-1100 aluminum and in 0.40 mm-thick-Type 304L stainless steel. The completed elements were surveyed for α contamination, leak detected by means of a vacuum test chamber and helium leak detector, weighed, radiographed, and visually inspected. The gamma ray intensity of each plate through the jacket was approximately 2.5 r/hr at 50 mm. The weight and contents of each specimen are as shown by Table X.

Table X. Weight and Contents of U^{233} Reactivity Specimens

Specimen No.	Gross Weight (g)	Core Weight (g)	Aluminum Weight (g)	Stainless Steel Weight (g)
U^{233}-1	172.866	147.626	5.240	20.000
U^{233}-2	171.971	146.708	5.286	19.977
U^{233}-3	170.231	145.213	5.155	19.863
U^{233}-4	170.825	145.740	5.140	19.944
U^{233}-5	172.501	147.548	5.128	19.825
U^{233}-6	173.690	148.576	5.270	19.844

b. SEFOR Critical Fuel Plates for TREAT Tests. Twelve 152 x 51 x 6-mm stainless steel-jacketed SEFOR critical fuel plates were completed for excursion testing in TREAT. The depleted uranium core plates were machined to provide varying end clearance between core plates and jackets. The excursion test will evaluate the effect of end clearance on the axial expansion of the fuel elements. Core plates and jacket components were manufactured and the elements assembled by the techniques that were developed for manufacturing SEFOR critical fuel elements for use in ZPR-III.

Chromel-alumel thermocouples were inserted in two fuel elements for temperature monitoring. Finished element dimensions were inspected by methods proposed for the quality assurance inspection of SEFOR fuel elements. Table XI shows test fuel element data.

Table XI. ZPR-III-TREAT Test Fuel Element Weights and Dimensions

Element Number	Core Weight (g)	Core Jacket Length Clearance (mm)	Fuel Element Length (mm)	Fuel Element Passed Parallel Planes Separated (mm)
601	654.930	0.051	152.65	6.35
602	656.451	0.051	152.63	6.22
603	658.629	0.051	152.55	6.22
604	653.073	0.038	152.58	6.22
605	655.257	0.051	152.60	6.22
606	652.040	0.051	152.55	6.22
607	649.334	0.102	152.65	6.22
608	652.305	0.102	152.60	6.22
609	648.740	0.102	152.55	6.35
610	647.401	0.102	152.50	6.22
611T*	652.084	0.178	152.55	No Test
612T*	647.688	0.178	152.58	No Test

*Thermocouple elements

D. General Fast Reactor Fuel Reprocessing Development

1. Advanced Processes

a. Evaluation of Beryllia Crucibles for Halide Slagging. In the development of high-temperature processes that employ molten halide fluxes for the extraction of plutonium and fission products from fast breeder reactor blanket material, it is important to know the degree of contamination of the processed material through reaction with crucible material. In a small-scale experiment, the beryllium concentration of uranium metal held for 1/2 hr at 1200°C beneath a melted $CaCl_2$-4.8 m/o UCl_3 salt phase in a slip cast beryllia crucible (94% of theoretical density) increased from an initial value of 0.5 to 40 ppm. In the absence of flux, a value of less than 10 ppm would be predicted.[4] The presence of flux evidently accelerates the reaction with the crucible. While it is believed that the low concentration of 40 ppm of beryllium will not have a deleterious effect on the fuel, this will have to be verified.

2. Materials and Equipment Evaluation

a. Corrosion Resistance of Type 405 Stainless Steel. A corrosion program is underway to evaluate the performance of various steels as container materials for pyrometallurgical process systems. The corrosion

[4]Feder, H. M., et al., Interaction of Uranium and Its Alloys with Ceramic Oxides, ANL-5765 (July 1957), p. 18.

resistance of Type 405 stainless steel to the system having a metal phase of 81.4 w/o Cd-10.9 w/o Zn-5.4 w/o Mg-2.3 w/o U and a salt phase of 50 m/o $MgCl_2$-30 m/o NaCl-20 m/o KCl has been investigated. This system is under consideration for use in a high-temperature extraction facility. The salt for this experiment was prepared by exposing it to a magnesium-cadmium solution and then filtering. The salt, after this pretreatment, was clear and colorless when molten, contained less than 0.005 w/o water-insoluble material, and analyzed 0.4 to 0.5 w/o oxygen by the BrF_3 procedure. The low water-insoluble content does not seem to be consistent with the relatively high oxygen values; this will be investigated further.

In this experiment, Type 405 stainless steel test coupons were mounted as four agitator blades on a single shaft, one blade at each of four positions: in the Cd-Zn-Mg-U metal phase, at the metal-salt interface, in the $MgCl_2$-NaCl-KCl salt phase, and in the vapor above the salt. During the corrosion test, which lasted 225 hr at 650°C, the samples were rotated slowly. Throughout the experiment, the vapor phase was purged with argon to sweep away any hydrogen or HCl which might have evolved from the melt.

The depth of corrosion of all coupons during this test was below the limit of detection, i.e., <0.5 mil. Although the exposure time was short, the test shows that Type 405 stainless steel has excellent promise of being a satisfactory container material.

In scouting experiments in which the salt was not pretreated by exposing it to a Mg-Cd solution, and in which the vapor phase was not purged, serious embrittlement and corrosion of Type 405 stainless steel occurred, especially in the vapor phase (see Progress Report for August 1964, ANL-6936, p. 26). It is planned to perform the next experiment without the purge to determine whether the decrease in attack in the vapor phase was due largely to the salt purification or to the sweeping away of hydrogen and HCl.

b. High-temperature Materials. A number of refractory compounds are being examined for possible use for the containment of uranium and uranium alloys. Screening is by examination of the effect of partial submersion of sample cylinders in molten uranium at 1400°C for 24 hr. Although preliminary testing has not been completed, ZrB_2, HfC, NbN, and TiN appear to be promising.

3. Eddy Current Induction Probe

Two eddy current induction probes of similar physical dimensions have been operated under the same conditions and at the same temperature (485°C) in cadmium of various depths to determine whether probes which are similar will have to be calibrated individually. The zero points

and the slopes of the curves for the two probes were different, indicating that each new probe will have to be calibrated prior to use.

In the operation of a probe over a period of several months, it has been noted that there is a drift in the bias voltage required to zero the instrument, so that it is necessary to recalibrate the instrument occasionally at one known depth and temperature. The other characteristics of a probe (the change in output signal with liquid depth at constant temperature and the change in output signal with temperature at constant depth) have been found to remain constant.

4. Decladding Studies for TV-20 Cladding

When a uranium-fissium or a uranium-plutonium-fissium fuel pin clad with vanadium-20 w/o titanium (TV-20) alloy is exposed to hydrogen at elevated temperatures (about 250°C-300°C), the fuel pin becomes hydrided and the cladding is broken up into small fragments (see Figure 9). In the experiment with the uranium-fissium pin described previously (see Progress Report for November 1964, ANL-6977, pp. 25-26), the ends of the TV-20 cladding were sealed by welding. In the current experiment

Figure 9. Residue Remaining after Hydriding and Dehydriding a Uranium-Fissium Pin Clad with Vanadium-20 w/o Titanium (TV-20) Alloy

(Lighter fragments are TV-20 cladding)
(scale shown is in centimeters)

with the uranium-plutonium-fissium fuel, the ends of the cladding were sealed by crimping. In both experiments, the cladding disintegrated in about 15 min after exposure to hydrogen at 2 atm. (However, periods of several hours are allowed to ensure completion of the hydriding of the fuel.) The enclosure of the fuel pin by the cladding alloy, the short time required for the disintegration of the cladding to occur, and the known permeability of hydrogen through vanadium suggest that the mechanism leading to the disintegration of the cladding might involve the diffusion of hydrogen through the TV-20 cladding and the hydriding of the fuel alloy, which results in an increase in pressure within the cladding sufficient to destroy it. After the uranium and plutonium hydrides have been decomposed by heat, they may be dissolved in a suitable salt-metal system.

In the current experiment, a U-20 w/o Pu-10 w/o fissium pin was used. The pin was 0.144 in. in dia. and was contained in a 0.17-in. ID TV-20 tube. The clad fuel pin was exposed to about 2 atm hydrogen pressure at 250-290°C for 20 hr. The hydrided uranium-plutonium-fissium was dehydrided under vacuum (at 300-400°C for about 4 hr) and was dissolved in a Cd-15 a/o Zn-15 a/o Mg metal phase in the presence of the LiCl-KCl eutectic by stirring for 10 hr at 600°C. The TV-20 tubing is thought to have been broken into small pieces but not dissolved by this procedure. Although final analytical results on uranium are not yet available, results indicate that 96% of the original plutonium was dissolved in the metal phase. This result, although lower than desired ultimately, is nevertheless encouraging.

In a separate experiment, the solubility of TV-20 cladding alloy in Cd-15 a/o Zn-15 a/o Mg metal alloy was determined by contacting the cladding alloy with the solvent metal for 24 hr at 600°C (including 8 hr of stirring). At the end of this period, the concentration of vanadium in the cadmium-zinc-magnesium alloy was below the limit of spectrochemical detectability (~0.01%), and the concentration of titanium was no greater than 0.01%. The very low solubility of the cladding alloy in the Cd-Mg-Zn alloy should make possible good separation of the cladding from the solution of fuel constituents.

E. Liquid Sodium Coolant Chemistry

The preliminary studies of the reactions of liquid sodium with common contaminants such as hydrogen, oxygen, and carbon, and the analytical development work to date have revealed a need for ultra-pure sodium. An intensive effort has been initiated to supply this need. Several approaches are being considered: distillation, filtration, hot gettering, centrifugation, and zone refining.

Previous solubility studies (see Progress Report for July 1964, ANL-6923, p.32) showed that vacuum-distilled liquid sodium held in contact with graphite had a carbon content which varied erratically. This suggested the presence of carbonaceous particulate matter capable of passing through the 5-μ-pore stainless steel filters used in sampling. More recently, vacuum-distilled sodium which was dissolved in water, acidified, and filtered through a fine (15- to 20-μ-pore) quartz glass filter, left behind a number of 20- to 200-μ-size dark particles. These relatively large particles probably formed during the dissolution as a result of agglomeration of smaller particles initially present in the sodium. X-ray diffraction analysis of the filtered particles showed only a halo, indicating that they were probably amorphous. Chemical analysis identified them as being carbonaceous. It thus appears that a considerable portion of the carbon present in sodium is in the form of particulate matter. The use of electron microscopy to determine the size of such particulates in solid sodium is being investigated.

Currently, attempts are being made to separate particulate carbonaceous matter from sodium by centrifugation. In the first centrifugation experiment, a sealed stainless steel capsule containing sodium (m.p. 97.5°C) was centrifuged at 2000 rpm at 200°C for 30 min in a small, specially modified clinical centrifuge. After quenching, however, no significant difference was found in the carbon content at the upper (180 ppm), center (140 ppm), and bottom (220 ppm) portions of the column of sodium. Longer centrifugation as well as filtration (with submicron-pore-size filters) and zone refining will be used in further attempts to remove particulate carbonaceous matter.

F. EBR-II

1. Removal of Oscillator Rod and Thimble

An unsuccessful attempt was made to remove the stuck oscillator rod (see Progress Report for December 1964, ANL-6997, p. 12) from the oscillator thimble by pulling and impacting on the oscillator rod while restraining the oscillator thimble. Only $1\frac{7}{8}$ in. of vertical movement could be obtained while pulling with a force of 1200 lb and impacting with a 7-lb weight over a 6-in. stroke. Further efforts to remove the stuck oscillator rod and thimble were deferred until the necessary fuel handling could be accomplished, which would permit unlocking the control rod thimble by rotation.

Prior to fuel handling, three special filter assemblies were inserted through the three Stellite sleeves in the reactor vessel cover in the positions previously occupied by control rod drives Nos. 7 and 9 and the oscillator drive. The oscillator rod had formerly been located in control rod position No. 8. After installation of the three filter assemblies, the nine remaining control rods were latched to their drives. The control rod lifting platform was left in the "down" position, and the primary pumps were then operated for approximately 18 hr. Full reactor flow was maintained for about $1\frac{1}{2}$ hr of this time; during the remaining time, the flow was 50%. During full-flow conditions, each filter was rotated through 360° so that sodium flow was induced over the flanged surface of the Stellite sleeve in the reactor vessel cover by a Venturi-type eductor built into the filter assembly.

The filters were removed, disassembled, and inspected. No debris was found that could be identified as coming from the failed oscillator drive ball bushings.

The auxiliary gripper plug was removed because access to the primary tank through the auxiliary gripper hole is required for subsequent work aimed at removal of control rod thimble No. 8, containing the oscillator rod and thimble.

Next, the reactor vessel cover lifting drive was installed, and the reactor vessel cover was raised. The nine control subassemblies were disconnected from their drives, and the control rod lifting platform was raised to the "up" position. The primary sodium was then heated to 580°F, and the fuel-handling equipment was checked out. After this, three row-8 outer blanket subassemblies were transferred to the basket and back to the reactor grid. Three round-trip transfers were also made, using a dummy steel subassembly between the temporary coffin and the transfer arm via the fuel-unloading machine. In the initial operation of the fuel-unloading machine, a bevel gear in the differential mechanism of the gripper drive

was broken. The gripper was at the same elevation in the transfer port tube where sticking has been observed in the past. The gear was replaced and the transfer port tube was cleaned with hot sodium.

The six subassemblies around the No. 8 control rod thimble were replaced with six thimble removal dummies, to permit unlocking of the control rod thimble. A special removal tool was inserted through the auxiliary gripper hole and attached to the No. 8 control rod thimble. With some difficulty the control rod thimble was unlocked from the reactor grid. It was then pulled into a special removal pipe, stored in a shielded storage pipe, and allowed to cool in an inert atmosphere. The maximum radiation level measured 16 in. away from the removal pipe was 450 R/hr.

The bottom ends of the control rod thimble and oscillator rod thimble were visually inspected and appeared to be undamaged. The assembly was cleaned prior to storage in the source coffin. The control rod thimble was lowered into the source coffin, and the removal tool was disengaged. Visual inspection verified that the oscillator thimble and control rod thimble were in the source coffin. What appeared to be a 1/8-in.-diameter steel ball is jammed between the oscillator rod and the oscillator rod thimble. Further inspection will be deferred until later.

The orientation bar which locks the control rod thimble in the reactor vessel grid was checked with two special tools. The first tool simulated the lower end of a control rod thimble with its bayonet slot for engaging the orientation bar. The tool was lowered into the primary tank and successfully locked onto the orientation bar in the reactor vessel grid. The second tool was used to measure the elevation of the center of the orientation bar with respect to the ends of the bar. This tool was lowered into the primary tank and verified that the bar was not bent downward in the middle. A new control rod thimble was installed through the auxiliary gripper hole in the reactor by use of the special handling tool which had been used for removal of the other thimble.

2. Inadvertent Raising of the Safety Rods

A decision was made not to raise the safety rods before the fuel-handling checkout until a check could be made to determine whether debris could cause malfunctioning of the drives. Therefore, a temporary wiring connection was made to bypass the safety rod "up" limit switches in the fuel-handling shutdown circuit. Because of a previously undiscovered circuit characteristic, the act of bypassing the "up" limit switch energized the safety rod drive circuit and raised the safety rods about 4 in. by the electrical drive. The manual safety rod drive, which had been partially connected in preparation for the pending safety rod checkout, resisted the upward movement of the safety rods, resulting in cracking of the sprocket hub in the manual drive mechanism. Following this, the safety rods were

lowered slowly by means of chain hoists attached to each shock absorber shaft. The lowering proceeded smoothly with no evidence of binding between the safety subassemblies and their thimbles. Measures are being taken to correct the circuits.

3. Plant Maintenance and Modification

The leak detector probes in the sodium-recirculation pumps were wired for annunciation on the Sodium Boiler Plant alarm panel.

To reduce pressure drop and provide more cooling water to the main secondary sodium pump, the supply piping for the cooling coils of the top and bottom stators has been modified for parallel flow rather than series flow through the coils.

The heater circuits for the secondary sodium plugging loop were rewired.

The siphon break control system for the primary purification loop was modified with the addition of a solenoid-controlled, air-operated valve in the argon line. The system was tested satisfactorily.

Modification of the secondary sodium pump control system was started. The amplidyne was replaced with a dc generator, a new control transformer was installed, and wiring changes were started.

A limit switch was installed on the new manual breathing valve in the emergency airlock, and a mantrap switch was installed. The airlock alarm was modified to include both of these items.

Miscellaneous small, molded-case circuit breakers and motor-overload relays were also tested with the new overload relay test unit.

Both the primary and the secondary sodium-purification systems remained frozen.

Installation of the block valves to the secondary sodium system plugging meter was completed. This system is now ready for service.

Helium leak testing of the vacuum system for the primary purification loop disclosed a cracked bellows in the isolation valve to the vacuum pump. This valve was removed and replaced with a length of pipe. Further leak testing showed the system to be tight. The purification system is now ready for service.

The new bellows for the expansion joint in the steam-bypass desuperheater line was received and installed in the line.

Piping and valves have been installed to provide for blowing down the sight glasses on the high-pressure flash tank and the No. 3 and No. 4 feedwater heaters.

A bypass valve was installed in the No. 1 riser of the cooling tower. It is now possible to bypass flow to the tower basin from both the No. 1 and No. 4 risers, increasing flexibility of operation.

The installation of a check valve in the 6-in. feedwater line to the steam generator was held up during the month, pending certification of welding electrodes. Certification was completed by Argonne, Illinois.

4. Fuel Cycle Facility

a. Cells. One of the more difficult remote maintenance operations in the EBR-II Argon Cell is the removal of a bridge drive motor from a crane bridge.[5] The drive motor is difficult to reach, and the removal operation must be viewed with a periscope in the cell wall. To carry out the removal step, a bridge-drive lifting tool was fabricated. The original design has been modified so that the operator can see whether or not the drive motor has been properly engaged by the lifting-tool hooks. The modified lifting tool was successfully used to remove a bridge drive motor from a crane bridge in the Argon Cell. No difficulties were encountered in this operation.

Drive units are used for driving the drive wheels of the two crane bridges in the Argon Cell. The units in current use employ new, improved planetary-gear reducers[6] that have replaced the ones that were originally installed, and which failed after a few hours of operation.[7] The gears in the new reducer unit were examined and found to be in excellent condition after a total in-cell operating time of 36 hr.

During investigation of the failure of an Argon Cell manipulator, it was found that a short circuit existed among several pins of a 64-prong male connector at the pivot tower above the center of the cell. This is reparable without affecting the cell atmosphere. Consideration will be given to replacing or eliminating these connectors.

In-cell lighting of the EBR-II Air and Argon Cells is provided by ninety-six 1000-W mercury vapor lamps.[8] This lighting has proved to

[5]Graae, J. E. A., Design of a Remotely Removable and Replaceable Crane-Bridge Drive Unit for the EBR-II Fuel Cycle Facility, ANL-6966.

[6]Planetary gear systems are compact and provide a large gear reduction in a limited space.

[7]Chemical Engineering Division Summary Reports for October-December, 1962 and July-December, 1963, ANL-6648, p. 100, and ANL-6800, p. 156.

[8]Chemical Engineering Division Summary Report, July-September, 1962, ANL-6596, pp. 99-101.

be very satisfactory. In the 30 months that they have been in use, no lamp has burned out. Most lamps have given about 17,000 hr of service. In the Argon Cell, which has 72 lamps, the illumination along the centerline of the cell working area has decreased from an initial value of 180 ft-candles in August 1962 to a value currently estimated to be about one-half of the initial value. (In February, 1963, this illumination value was 125 ft-candles.) Preparations are being made to start replacing lamps.

An argon-atmosphere enclosure system[9] is being installed in the Chemical Engineering Division at Argonne, Illinois, in order to test the effect of a dry argon environment on the operation of equipment and to demonstrate processes for use in the EBR-II Argon Cell. One of two gloveboxes and an argon-purification system were previously installed and placed in operation (see Progress Report for May 1964, ANL-6904, p. 47). The argon-purification system is similar to that used in the EBR-II Argon Cell. The second glovebox has now been installed and placed in operation. Currently, it is being used by the Remote Control Division for carrying out tests on fuel-decanning equipment. Following these tests, the Chemical Engineering Division plans to conduct tests on electrical motors, bearings, and other equipment.

The construction of an inert-atmosphere glovebox, 24 ft long by 12 ft wide by 14 ft high, is nearing completion (see Progress Report for November 1964, ANL-6977, p. 31). The interior surfaces are being painted, after which additional plant-scale prototype process equipment will be installed and leak tests made. Within the enclosure, a previously installed one-ton capacity crane has been successfully tested for control of hoist and trolley speeds with varying loads up to the capacity of the crane.

b. Fuel Recovery and Fabrication. The Argon Cell decanner, modified by the addition of a tilting scrap separator tube, was used to decan and chop 57 elements with only minor difficulties. An ingot of unirradiated enriched fissium alloy was cast in a 93% yield from an 11.7-kg blend of scrap fully enriched uranium plate, material of 1.25% enrichment, and fissium elements.

All 184 fuel rods rejected during the reclamation of elements recovered by disassembly were decanned; 122 were remeasured in the pin processor, and 78 were chopped for remelting. Of the accepted pins, 44 were reassembled along with 78 unirradiated rods previously fabricated. Forty-five of the latter were leak tested, bonded, and bond tested, yielding 37 acceptable elements. The 36 acceptable irradiated fuel rods from the first assembly discharged from the reactor were assembled, welded, leak tested, bonded, and bond tested to yield 22 acceptable elements ready for final assembly. It is expected that yields at all these steps will be much improved as experience is gained.

[9]Chemical Engineering Division Semiannual Report, January-June 1964, ANL-6900, pp. 114-117.

Two control rods were assembled from fuel rods obtained previously. The new assembly straightness-testing machine and straightener have been placed in the Air Cell and is being readied for use.

A machine to decan the blanket elements contained in the core, outer, and inner blanket subassemblies is being designed. The machine will consist of transfer magazines, a cutting unit, an ejector unit and a sampling unit. After the blanket elements have been removed from their subassembly by the dismantling machine, they will be loaded into magazines and transferred into the Argon Cell. The cutting operation will remove the ends of the element and reduce the remaining portion of the element to short lengths of uranium rod and sheath. A cylindrical heater will be used to melt the sodium bonding between the rod and cladding after which the rod will be pushed through an orifice to eject it from the tubular sheath. A mechanical master-slave manipulator will be used to perform all of the handling operations.

An experimental cutting unit and ejector unit were used to decan 30 sodium-bonded blanket elements in a dry argon atmosphere. The cutting unit consisted of a rolling cutter wheel which is held against the blanket element by two knurled rollers. As the knurled rollers are rotated, the cutting wheel severs the blanket element cladding.

c. Skull Reclamation Process. A skull reclamation process[10] is being developed for the recovery and purification of the fissionable material that remains in the melt refining crucible after a melt refining operation. Work is continuing on the engineering development of plant-scale equipment and process procedures for the oxidation and retorting steps of this process.

Fabrication of a prototype (M-2) skull oxide reclamation furnace and auxiliary equipment is continuing (see Progress Report for December 1964, ANL-6997, pp. 15-16). While the M-2 furnace is being constructed, the M-1 furnace is being used for component testing. The hinged, resistance heater units for the M-2 furnace have been received from the manufacturer and installed. The fabrication status of auxiliary furnace equipment is as follows:

1. The following have been recently completed: (a) a molybdenum-30 w/o tungsten transfer line for transferring flux and metal phases out of the tungsten crucible. (b) a lifting tool for removing a loaded tungsten crucible from the M-2 furnace. (c) a charge bucket and hopper for charging material to the crucible within the furnace.

2. A charging chute, which will be inserted through the charging port and will serve to protect the stirring impeller during the charging step, is nearing completion.

[10] Chemical Engineering Division Semiannual Report, January-June 1964, ANL-6900, pp. 52-64 and 120-125.

Equipment components for the M-2 furnace have been tested with molten metal in the M-1 furnace. These tests have evaluated the mixing performance of a four-bladed Mo-30 w/o W stirrer with blades pitched at a 45° angle and the transfer capability of the M-2 furnace transfer line [see Item 1 (a) above] for transferring molten metal from a crucible in the furnace to an outside container. For the tests, a 70-kg charge of zinc was melted (575°C) under reduced pressure (1-2 psig argon) in a plant-scale pressed-and-sintered tungsten crucible. For the mixing tests, the stirrer was rotated to discharge the crucible contents downward and was used with a previously reported agitator stuffing box assembly (see Progress Report for October 1964, ANL-6965, pp. 28-30). The stirrer was operated with the impeller submerged 1/2 in. below the surface of the zinc at various speeds up to 740 rpm to measure stirrer-motor power requirements. At 740 rpm, the power required was 1/3 hp. [In an earlier test with molten lead, good agitation with a similar type impeller was achieved at a mixing speed of 775 rpm and a power requirement of 3/4 hp (see Progress Report for July 1964, ANL-6923, p. 38).]

After the mixing tests, the molten zinc was transferred through a preheated (600-700°C) transfer line by pressurizing (14 to 15 psig argon) the furnace. The discharge end of the transfer line was connected to a sealed receiver vessel which contained an 8-gal steel (22 ga) pail. (Similar light-gauge, steel pails will be used as the primary container in the Fuel Cycle Facility for the disposal of wastes from the process.) The transfer of the zinc (95 w/o of the original charge) to the pail was carried out smoothly and rapidly (within 2½ min). The zinc product adhered to the bottom of the pail; however, there was no evidence of dissolution of the steel. Very little zinc heel was found at the bottom of the tungsten crucible. Some zinc had splashed up to the upper portions of the crucible and stirrer, which may have been caused by either agitation or splashing during an argon backpurge of the transfer line.

A preliminary test of the plant-scale retort (see Progress Report for December 1964, ANL-6977, p. 18) was carried out. In this test, a 10-kg charge of zinc-magnesium was successfully distilled from a graphite crucible (enclosed by a graphite retorting assembly[1]). The Zn-Mg was distilled with very little loss; less than 100 g escaped through the graphite retorting assembly. All parts of the retorting apparatus were readily disassembled; no sticking of components was encountered.

d. Fuel Surveillance. A number of devices are being provided to facilitate inspection and evaluation of the fuel and fuel assemblies which will be removed from the reactor at progressively increasing burnup. A fuel-element holder is being installed in the Air Cell, which will be used in conjunction with a collimator and a scintillation counter outside the cell to scan the element and to determine relative burnup as a function of position.

A wire clipper and micrometer have been provided to measure the diameter of cans and detect incipient swelling.

Provision is being made to illuminate adequately the lower part of an irradiated assembly in the Air Cell to permit examination and photography.

Testing and installation of a mechanism for puncturing fuel element cans and for measuring pressure and volume of the gas contained is continuing. A vessel has been provided in the Air Cell to remove sodium from selected decanned irradiated rods so that they may be returned to the Argon Cell for remeasurement in the pin processor, and for detailed examination and photography.

G. FARET

1. General

Progress on the various design packages of Title II beyond that reported previously (see Progress Report for December 1964, ANL-6997, p. 19) is as follows:

Package II - Reactor Vessel - complete.

The reactor vessel procurement selection board has made a formal vendor selection recommendation to the AEC. This recommendation is now being considered by the Commission. In the interim period, the Laboratory is reviewing the reactor vessel design for potential areas of cost reductions which may result from design detail changes. Primary attention is being directed toward those design detail changes which may effect fabrication economies without significantly affecting performance of the vessel.

Package III - Liquid Metal Heat Exchangers - This package is being issued for construction.

Package IV - Liquid Metal Pumps - The Laboratory's comments on this design package have been reviewed by the Architect and are being incorporated into the final package.

Package V - Control and Instrumentation - This package is being reviewed at the Laboratory. Formal comments are being prepared per the usual procedures.

Package VI - Special Piping Materials and Valves - Final issue of this package is expected in the near future.

Package VII - Special Early Procurement Items - Laboratory comments on this package (except for the wet fuel storage tank) have been reviewed with the Architect. Initial issue of drawings and specifications of the wet fuel storage tank has just recently been submitted for Laboratory review. This completes the Architect's issue of this design package.

Package IX - General Design - Drawings and specifications for a major part of this package have just been received by the Laboratory. Some late design items, including the following, have been scheduled for completion by the end of March, at which time the entire package is scheduled for final issue:

1. shield cooling system;
2. cavity structure and instrument thimbles;
3. cell details;
4. access air locks;
5. argon cooling system;
6. fuel-transfer hoist and carrier equipment;
7. sodium-sampling systems;
8. sodium-purification systems;
9. blanket gas vent connections;
10. NaK annulus pump suction details.

Package IX is being reviewed on a high priority.

2. Neutron Shield

A detailed study and evaluation of the design of the reactor radial neutron shield and energy-absorption structure (described in the Progress Report for October 1964, ANL-6965, p. 32) failed to provide the degree of confidence in reliable, long-term performance necessary for acceptance of the design. In particular, the thermal conductivity of serpentine concrete appears to deteriorate to an unacceptable low value with time and temperature. As a result, high temperature gradients in the concrete can cause loss of water and subsequent structural deterioration.

Other shield configurations are being evaluated. The most feasible method now under study appears to be the use of stainless steel-clad, borated graphite within the reactor vessel with an ordinary, external, concrete, radial energy-absorption structure surrounding the vessel proper. Although the effects of this change are yet to be completely determined, it has certain advantages. For example, the major heat-producing portion of

the shield will be within the vessel, where cooling can be readily affected. As a corollary, little heat is generated beyond the vessel limits and the heat load on the cavity cooling system is substantially reduced. Moreover, relatively low temperatures should exist in the radial energy-absorption structure.

3. Safety Analysis

Meetings have been held with both the Division of Regulations and Licensing (DRL) and with the FARET Review Subcommittee of the Advisory Committee for Reactor Safety (ACRS). The Laboratory is now preparing a response to questions raised as a consequence of these reviews.

4. Shielded Windows

The first step of the hydraulic pressure test has consisted of assembling the test fixture in the horizontal position and obtaining a leak-tight assembly. The $8\frac{1}{2}$-in.-thick glass slab was installed in its frame and partially caulked with lead wool to prevent shifting of the glass when the fixture is placed on end for the hydraulic test. The framed glass was then installed into the fixture. At this point, it was found that the gasket would not seal at one corner; furthermore, the gasket area of the test fixture, which had been machined prior to welding the steel side walls in place, was 0.030 in. out of flat. After remachining with an end mill, the peripheral gasket area flatness variation of 0.003 in. was accepted. On reassembly, the weight of the glass alone appeared sufficient to compress the gasket uniformly and thus make an effective seal. In addition, the gasket was compressed by tightening the glass frame bolts to 40 ft-lb of torque. A steel cover was installed so that the fixture could be pressurized. An air pressure of 6 psi was held for a period of a week without perceptible pressure loss.

Strain gauges have been applied to the glass slab and a fixture for measuring strain during the next phase of the planned hydraulic pressure test has also been attached.

5. Control Rod Drive Seal Tests

Test facilities for the sliding seal and bellows seal (see Progress Report for March 1964, ANL-6880, pp. 44-45) have been designed and fabricated (see Figures 10 and 11). Both test facilities include a ball-nut screw mechanism for driving a simulated control rod drive shaft through a 3 ft stroke. A sodium reservoir which will contain 1200°F sodium completes the facility. In addition, the sliding seal test facility includes a scram feature to test the compatibility of the drive shaft scram position static seal.

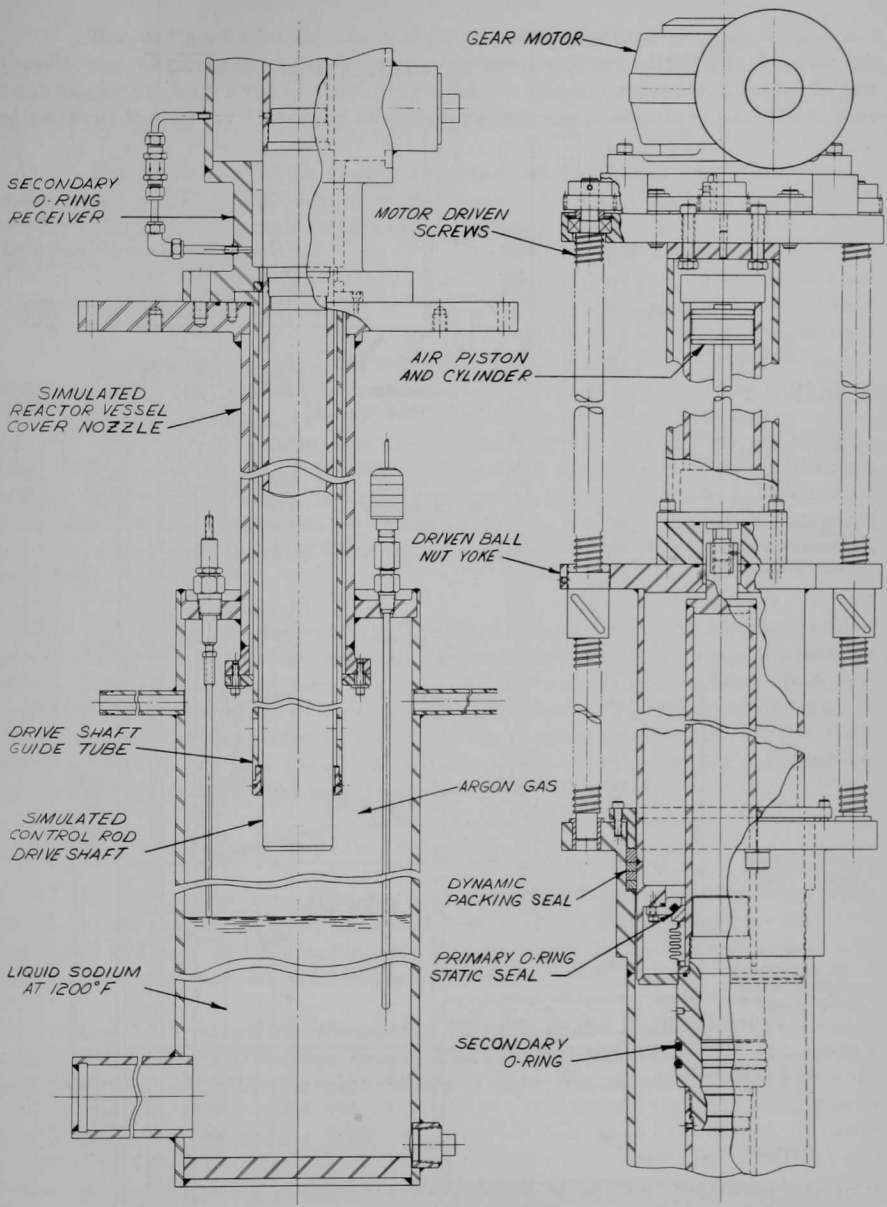

Figure 10. FARET Control Rod Drive Mechanism Sliding Seal Test Apparatus

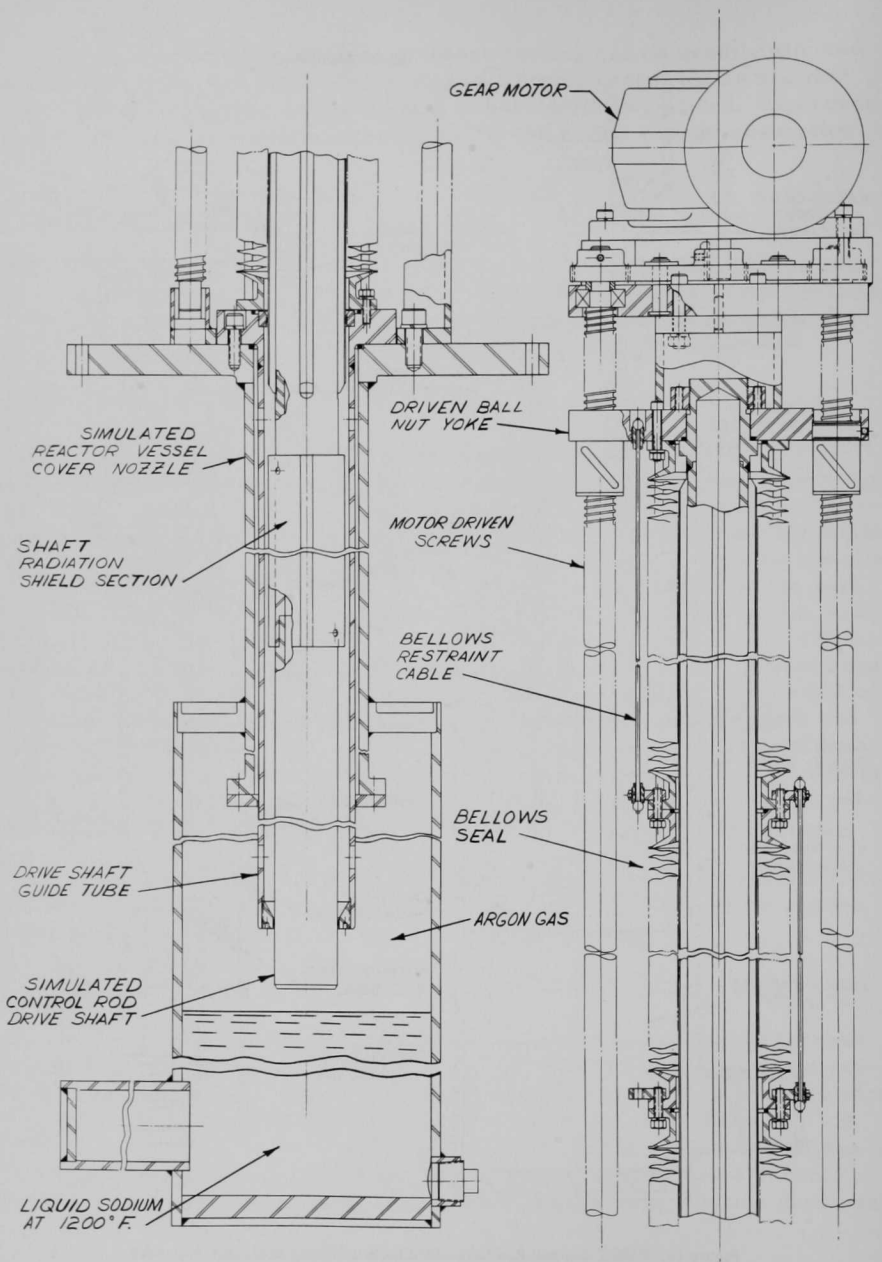

Figure 11. FARET Control Rod Drive Mechanism Bellows Seal Test Apparatus

The bellows seal was leak tight as demonstrated by helium leak-testing and is being brought to operating temperature (1200°F). The sliding seal assembly had a faulty "O" ring seat. A minor revision is being made to correct the upper "O" ring seal before the reservoir is filled with sodium.

The bellows will be cycled continuously by means of the simulated drive shaft with 1200°F sodium in the reservoir. It is planned to inspect the bellows leak tightness continuously and inspect for sodium buildup at least once each month.

6. Fuel Slip-fit Experiment

The uranium oxide (~3% enriched U^{235}) sample of the slip-fit fuel element under test in the CP-5 reactor (see Progress Report for December 1964, ANL-6997, pp. 23-24) was removed from the reactor after irradiation for one month. Essentially, the centerline fuel temperature did not change from the original value of 1030°C. At the time of removal, the temperature was 1070°C. The cladding temperature increased from 210°C to 215°C. Indications are that the power increased slightly, probably because of an increase in neutron intensity near the capsule by virtue of a control rod movement.

The 3-mil gap between the fuel and capsule was filled with argon gas in the above irradiated capsule. A replacement capsule was assembled identical in all respects with the first capsule except that helium replaced argon. Upon irradiation of this capsule, the centerline temperature was 720°C and the cladding temperature 210°C. This difference (310°C) indicates that the type of gas in a small gas-filled gap (0.003 in.) can be expected to influence significantly the heat transfer across the gap.

7. Fuel Assembly Sodium Flow Test Loop

a. Construction. The pressure vessel, dump tank, and expansion tank for this loop have been installed. Most of the piping, duct to the scrubber system, and electrical wiring (including Calrod heaters) are complete. Thermal insulation is being applied.

b. Instrument Development. Testing of the Baldwin-Lima-Hamilton high-temperature full-bridge gauges has been initiated to learn of attachment problems and behavior characteristics of high-temperature gauges.

8. Core Support Analysis

Strength and deformation analysis was started on the two-plate grid support structure of the FARET reactor. Preliminary analytical results have been obtained for some geometry-load combinations of the structure. Other results with different combinations are to follow.

II. GENERAL REACTOR TECHNOLOGY

A. Experimental Reactor and Nuclear Physics

1. Cherenkov Counting of Aqueous Solutions

A Cherenkov detection system used recently in experiments with aqueous solutions is shown in Figure 12. In this system a 12-ml sample vial containing the active solution is placed between two low-noise EMI 6255S quartz phototubes. The vial is coupled to the tubes by either water or silicone fluids. A 100-nsec total-coincidence gate circuit is used to reject background noise. A 3-in. NaI(Tl) crystal is used to view the sample and detect beta-gamma coincidences. With Mn^{56} as a source and thin-walled glass or quartz vials, counting efficiencies up to 39.8% can be attained. These measurements, taken as a function of the concentration of $MnSO_4$ in water, are shown in Table XII. By comparison with previously determined liquid scintillation results,[11] it was found that approximately 7.5% of the system efficiency results from gamma rays detected in the Cherenkov channel. All counting was done at room temperature and where the beta background was about 1.2 cps.

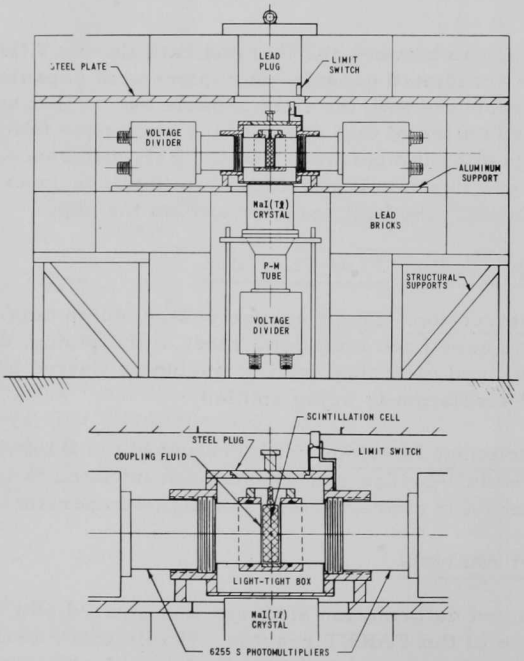

Figure 12. Cherenkov Counting System

[11] DeVolpi, A., and Porges, K. G. A., Mn^{56} Coincidence Counting Facility, ANL-6760 (Aug 1963).

Table XII. Cherenkov Detection Efficiency versus Concentration

Concentration* (g) $MnSO_4$/liter	Total Counting Efficiency (%)
0	39.8
50	37.6
100	36.2
200	34.2
300	32.1

*With 50-λ aliquots of Mn^{56} added to each sample.

The counting efficiency obtained when measuring Cherenkov emission from activity dissolved in water was compared with that obtained when measuring scintillations resulting from activity dissolved in scintillator solution. A $Na^{24}NO_3$ source dissolved in water (at a concentration of approximately 580 g of $NaNO_3$/liter) was counted with 25% efficiency. In contrast, 96 and 99% efficiencies were obtained, respectively, when a $Na^{24}NO_3$ source at a concentration of approximately 25 g of $NaNO_3$/liter and a $Mn^{56}SO_4$ source (approaching zero concentration) were dissolved in a liquid scintillator mixture of ethanol-water-dioxane-napthalene. Thus, higher counting efficiencies can be achieved by dissolving the activity into scintillator mixtures.

2. Fast-neutron Hodoscope

A monitoring device which provides both the time and spatial history of fuel movement is now in an advanced stage of development for use in TREAT (see Progress Report for December 1964, ANL-6997, p. 30). This hodoscope is expected to provide 1-msec time resolution, 0.32 by 1.3-cm space resolution, and adequate signal-to-background discrimination of fast fission neutron detection emanating from the fuel. This system is designed to be a forerunner of a 320-channel system capable of viewing large clusters in a meltdown loop.

A 50-channel collimator focused on an area of about 5 x 30 cm at the fuel plane in the center of the reactor core is being constructed of tapered steel plates with machined slots.

Development work continues on various aspects of noise pickup, photographic readout efficiency, a real time indicator, and actual testing under meltdown conditions.

B. Theoretical Reactor Physics

1. ZPR-VII Data Analysis

A study is being made of the effect of using various formulae for the escape probability P_0 in the calculation of resonance integrals for slab lattices. Calculations have been completed for slabs of U^{238} which are 0.5 cm thick and separated by thicknesses of water of 0.2, 0.5, and 1.0 cm. The resonances of U^{238} having the ten largest values of I_∞ were considered for room temperature in the framework of the NRIA approximation,[12] in which the resonance integral is given by

$$I = \frac{\sigma_0 \Gamma \gamma}{E_i} L'(Z'', \xi) = \frac{\sigma_0 \Gamma \gamma}{E_i} \int_0^\infty P_0(Z'', \psi)\, \psi(\xi, x)\, dx.$$

The formulae used for P_0 in the evaluation of L' by numerical integration are given below:

Exact: $$P_0^E = \frac{1}{x} \int_0^1 \frac{\mu(1 - e^{-x/\mu})(1 - e^{-y/\mu})\, d\mu}{1 - e^{-(x+y)/\mu}};$$

GAM-I: $$P_0^G = P_0^I\left(\frac{x}{1 - C}\right), \text{ where } P_0^I(x) = \frac{1}{x}\left[\frac{1}{2} - E_3(x)\right];$$

Nordheim: $$P_0^N = \frac{P_0^I(x)}{1 + \left(\frac{2C}{1 - C}\right) x P_0^I(x)};$$

Wigner: $$P_0^W = \frac{1}{1 + \left(\frac{2x}{1 - C}\right)}.$$

Here, $x = \Sigma_1 a$ and $y = \Sigma_2 b$, where Σ_1 and Σ_2 are cross sections, and a and b are thicknesses of fuel and H_2O, respectively. The Dancoff factor is $C = 2E_3(y)$.

Table XIII lists the % errors in the resonance integrals.

Table XIII. % Errors in Resonance Integrals

	Lattice		
P_0	0.2 cm H_2O	0.5 cm H_2O	1.0 cm H_2O
Exact	0.00	0.00	0.00
GAM-I	+1.34	+0.23	-0.07
Nordheim	-2.39	-1.61	-0.74
Wigner	-4.46	-5.47	-5.74

[12] Adler, F. T., Hinman, G. W., and Nordheim, L. W., The Quantitative Evaluation of Resonance Integrals, Proc. 2nd UN Intnl. Conf. on Peaceful Uses of Atomic Energy, Geneva, Switzerland, Vol. 12, pp. 383-396.

C. High-temperature Materials

1. Preparation of Uranium Monosulfide

Further attempts were made to prepare US by a modified version of the electrolytic method used to make ThS.[13] The experimental procedure involved the electrolysis of a fused salt mixture containing NaCl-KCl eutectic, CaS, and UCl_4.

Efforts to eliminate oxygen contamination in the product by careful drying of the starting materials were unsuccessful. Drying precautions included vacuum calcining of the CaS at 1200°C, vacuum drying of the chlorides for several weeks at 100°C, and predrying of the melt by both purging with HCl gas and electrolysis. In addition, all sample preparation procedures except weighing were carried out in a glovebox. Although these measures seemed helpful in reducing contamination, the product was chiefly UOS. In comparison, the products of earlier runs under less stringent drying conditions, consisted of mixtures of UO_2 and UOS.

An additional complication arose from attack of the graphite crucible during electrolysis. When an attempt was made to purify the UOS by vacuum distillation of the excess salts at 1800°C, the carbon contamination reacted to form a large amount of UC_2.

The experimental results to date indicate that extensive modifications of the experimental procedure would be required to produce good quality US. Some of these are:

a. setting up the complete apparatus in a glovebox;

b. preparation of high-purity CaS and UCl_4 for use as starting materials;

c. finding and using a nonreactive crucible material

d. purification of the NaCl-KCl eutectic by a procedure similar to that used in the electrorefining of uranium.[14]

However, putting these modifications into effect would defeat the purpose of this research, which was to find a more convenient method than the gas-reaction one presently in use. Therefore, no further electrolysis experiments will be undertaken.

2. Properties of (Th-U-Pu) Phosphides

Sintering studies of UP have continued with emphasis on grain growth as a function of time and temperature. A plot of the log of grain size versus

[13] Didehenko, R., and Litz, M., Preparation of Lanthanide and Actinide Monosulfides by Fused Salt Electrolysis, J. Electrochem. Soc. 109, 247-250 (1962).

[14] Hill, D. L., Perano, J., and Osteryoung, R. A., An Electrochemical Study of Uranium in Fused Chlorides, J. Electrochem. Soc. 107, 698-705 (1960).

the log of time yielded a straight line. A plot of the log of grain size versus the reciprocal of temperature also was linear. Nonetheless, grain growth as a function of either temperature or time was not extensive. Samples fired for one hour at 2200°C, or for 5 hr at 2000°C, exhibited an average grain size of about 15 μ, whereas the original UP had a size of 2.5 μ.

Vaporization of UP in vacuum was investigated in the temperature range from 1600 to 2200°C. Weight losses were virtually negligible at 1600°C, but became pronounced above 2000°C. Small pellets lost 3% of their weight per hour (1.6×10^{-5} g/cm^2/sec) at 2200°C. A plot of the log of weight loss/cm^2/sec versus the reciprocal of temperature yielded a straight line.

UO_2 commonly occurs as a secondary phase in UP as a result of oxygen contamination, and an understanding of its effect on the overall properties of UP compacts is important. X-ray diffraction and metallographic analysis revealed little or no solid-state interaction between UP and UO_2. No evidence of an intermediate phase was detected, and the lattice constants of the two compounds were unaffected by the presence of the other. Vaporization studies conducted at 2000°C in vacuum revealed that UO_2 lost weight at a faster rate than UP, and that vaporization of intermediate compositions was accelerated, partly because of the high-temperature reaction $UP + UO_2 \rightarrow 2UO\uparrow + P\uparrow$. Densities of 95% of theoretical and higher were obtained for samples across the entire compositional range.

The densification of PuP in an atmosphere of flowing argon was studied to determine the best sintering temperatures. Previous attempts to sinter PuP in vacuum resulted in a maximum density of about 88% of theoretical and a weight loss of about 2%. The density and percent weight loss of PuP pellets sintered at temperature intervals of 100°C for a period of two hours are shown in Table XIV. The argon atmosphere reduced vaporization and pellets were sintered to a maximum density of 93% of theoretical with less than 1% weight loss including 0.5 w/o binder.

Table XIV. Density and Weight Loss of PuP Pellets Sintered under Argon at Temperature Intervals of 100°C for Two Hours

Sintering Temperature (°C)	Density (% of Theoretical)	Weight Loss (%)
1400	68	0.48
1500	74	0.52
1600	80	0.57
1700	85	0.67
1800	92	0.81
1900	93	0.91
2000	93	1.10

3. Mechanical Properties of Uranium Compounds

Fracture tests with specimens of UO_2 have been carried out at 1500°C, 1750°C, and 1900°C. The trends reported previously (see Progress Report for November 1964, ANL-6977, pp. 52-53), namely, the increased plasticity upon raising the temperature from 1000 to 1250°C, and again to 1500°C, continued at an accelerating rate in proceeding from 1500 to 1900°C. The latter represents the maximum temperature at which meaningful tests can be carried out, since volatilization of the UO_2 in the vacuum chamber (pressures of the order of 6×10^{-6} Torr) becomes measurable within the time of test (15 to 20 min). Slow strain tests were not conducted for this reason (time of test 50 to 60 min).

Load-deflection curves obtained at these higher temperatures show similar characteristics: an elastic portion; a well-defined yield point; and a rise to maximum stress, followed by a fall as cracks form and propagate within the material. The elastic limit drops with rise in temperature and with slower strain at a given temperature. The yield point becomes more extended with rise in temperature, and with slower strain. Serrated yielding, as observed in ductile face-centered cubic metals, becomes characteristic of UO_2 (also cubic) at and above 1500°C, indicating that numerous slip systems become operative. Final fracture commences as a ductile intercrystalline type, extending through a major portion of the section, followed by a brittle, partly intercrystalline, partly cleavage, fracture at the compression face. At 1900°C, only a thin surface skin carries the final load and suffers brittle fracture.

At these higher temperatures, a modulus of rupture has little meaning, owing to the extensive plastic deformation. The maximum stress, calculated by a similar procedure, is therefore reported, rather than breaking stress. Similarly, strain rate is reported in preference to load rate. Load rates actually used in the tests were identical to those of previous tests, varying from slow to fast in the ratio 1:10:20. The strain rate was calculated over the whole test, and the total strain is incorporated in Table XV.

Table XV. Mechanical Test Data for UO_2

Number of Samples in Batch	Density (g/cc)		Maximum Stress (kg/cm^2)		Mean Strain Rate (mm/sec x 10^4)	Mean Total Strain (mm)	Temperature (°C)
	Mean	Standard Deviation	Mean	Standard Deviation			
5	10.45	0.05	1017	95.2	1.23	0.29	1500
5	9.86	0.04	916	118.0	1.36	0.66	1500
4	10.34	0.05	1245	146.0	9.40	0.41	1500
5	10.04	0.10	1306	156.0	16.00	0.18	1500
5	9.65	0.10	1013	165.0	14.50	0.21	1500
5	10.50	0.07	479	99.7	2.95	0.89	1750
5	10.44	0.02	709	156.0	12.45	1.07	1750
5	10.61	0.002	1655	534.0	29.00	3.18	1750
4	10.60	0.01	752	94.9	13.46	2.21	1900
4	10.60	0.02	914	35.6	31.10	3.56	1900

4. Thermal Stability

Further calibrations with MgO in high-temperature, low-pressure environments have been made (see Progress Report for October 1964, ANL-6965, p. 57). Samples have been exposed to several time-temperature treatments to determine the rate of grain growth and activation energy. Grain-size measurements are in progress.

Samples of UO_2 have been prepared for use in evaporation rate measurements. Disc samples, approximately 5 mm diameter and 1 mm thick, are being used. Characterization of the materials through grain size, density, O/U ratio, and purity measurements is now in process.

5. Anelasticity of Some Uranium Compounds

In determinations of Young's modulus and internal friction of UO_2 (see Progress Report for November 1964, ANL-6977, p. 53) Poisson's ratio of 0.30 was used throughout the calculations. The data obtained are shown in Table XVI. The measurements were repeated several times, and the results were very consistent.

Table XVI. Dimensions, Density, Elastic Modulus, and Internal Friction of UO_2 at Room Temperature

Sample	Width (cm)	Depth (cm)	Length (cm)	Weight (gm)	Density[1] (gm/cc)	E_f[2] (kilobars)	E_e[3] (kilobars)	Q^{-1}[4]
1	0.564	0.417	6.459	15.9332	10.53	2056	2070	2.03×10^{-4}
2	0.538	0.480	6.350	17.2532	10.54	2062	2062	-
3	0.320	0.153	7.387	3.7107	10.45	1884	-	8.4×10^{-4}
4	0.322	0.320	6.784	7.4299	10.73	2067	2067	4.02×10^{-4}

[1]Density was determined by the displacement method.
[2]Young's Modulus calculated from the flatwise flexural vibration.
[3]Young's Modulus calculated from the edgewise flexural vibration.
[4]Internal Friction.

Samples have been prepared for studying the effect of the grain size on Young's modulus and internal friction.

6. Corrosion by Liquid Metals

a. Polarization Studies in Liquid Metal Environment. Two apparent causes of uneven current distribution in polarization tests were investigated: (a) the occurrence of relatively bare areas of small diameter on zirconium surfaces otherwise blackened by exposure to oxygenated sodium at 540°C, and (b) the phenomena occurring at the liquid-vapor interface region of the zirconium electrode shank.

Production of uniformly blackened sample surfaces was attempted by varying surface preparation prior to test. Machining, grinding,

and chemical polishing were tried separately and in combination, without success. However, during an investigation of impurity hydrogen as a possible cause of spotting, an appreciably more uniform result was obtained. Vacuum extraction of gas through the wall of a nickel tube immersed in sodium at 650°C was attempted and hydrogen has been tentatively identified as a component of the extracted gas. Afterwards a sample electrode was exposed to the treated (vacuum extracted) sodium for the normal period (20 hr) at 540°C. The immersed sample surface became uniformly coated with black film, there being some evidence suggesting the earlier existence of lighter spot areas. The investigation of the possible effects of impurity hydrogen is continuing, and the result described cannot yet be attributed definitely to hydrogen.

The possibility of intermittent cell shorting by relatively oxygen-free sodium condensate at the liquid-vapor interface region of zirconium electrode samples has been reported. Such shorting may interfere with polarization studies and may contribute to the nonuniform behavior of unpolarized samples by promoting self-polarization (given the thermal gradient that exists in the sodium). Vapor condensation on the electrode has been reduced by means of a local heater on the electrode in the vapor phase region, the heater maintaining a shank temperature somewhat higher than that of the surrounding vapor. An additional measure employed has been preoxidation (in oxygen) of the electrode shank surface to insulate electrically the shank area prior to the polarization study of the uncorroded end region in oxygenated sodium. The combination of these techniques may achieve the specific result desired. However, the insulating (at room temperature) property of the preoxidized area is not retained in the vapor region just above the sodium surface, although it is retained above and below this region. The phenomenon has been reproduced.

Investigation of the stripping of zirconium-corrosion film in sodium-calcium solution has continued. The dark or black appearance of corrosion films formed on unalloyed zirconium electrodes in oxygenated sodium at 540°C may be altered to that of a metallic character by exposure to sodium-calcium at 600°C. The alteration has not been completely achieved on samples whose corrosion weight gains had been relatively high. The interpretation that the corrosion product is reduced by the sodium-calcium solution appears to be correct.

Attempts to etch away the reduced material without loss of base metal have not been successful in the case of the unalloyed electrodes. This has been accomplished with zirconium alloy samples precorroded in steam. The relatively thicker films were partially reduced by the sodium-calcium treatment.

However, an approximate indication of the amount of oxide present on a corroded electrode may often be obtained through use of the

sodium-calcium treatment. If it is assumed that the corrosion-product oxygen (but not the corrosion-product zirconium) is removed by the sodium-calcium, and if correction is made for any bare sample area contacting the sodium-calcium (clean samples having been shown to gain weight moderately in sodium-calcium), a prediction of the result of sodium-calcium exposure may be made on the basis of weight-gain data. The prediction is usually in reasonable agreement with the result, which tends to support the validity of the original weight-gain data as a measure of the amount of corrosion that has occurred. For those cases in which good agreement was not obtained, one might suspect, for example, appreciable loss of corrosion product during exposure or absorption of a component of the liquid-metal solution by the sample metal.

b. Dissolution Kinetics in Liquid Metals. Preliminary to future work with sodium, solubilities of tantalum in liquid tin have been obtained over the temperature range from 600 to 1000°C. Ultrahigh-purity, zone-refined tantalum wire was equilibrated with liquid tin in a Vycor crucible for periods of from 48 to 100 hr at temperatures of 600, 700, 800, 900, and 1000°C. The longer equilibration times were used at the lower temperatures to insure saturation. Several 2- to 3-gm samples of the liquid were obtained at each temperature with the use of Vycor sampling tubes. The Sn (Ta) samples were analyzed for tantalum by a neutron-activation method.

The solubility data, in units of μg Ta/g Sn, obtained from the four irradiations can be represented by the equation

$$C_{Sn}^{Ta} = (2.274 \pm 0.214) \times 10^4 \exp\left[\frac{-(7{,}210 \pm 870)}{T°K}\right].$$

The overall heat of solution of tantalum in liquid tin is 14,320 ± 1,730 cal/mole. The 95% confidence limits for the data are indicated.

c. Lithium Corrosion at Elevated Temperatures. The study of corrosion behavior of refractory metals in lithium at temperatures higher than 1000°C has been continued (see Progress Report for November 1964, ANL-6977, p. 56). At 1100°C, the lithium-containing high-purity tantalum capsule suffered severe transgranular penetration after 100 hr of exposure. The maximum depth of attack in the liquid lithium region was 0.14 mm. In the liquid-vapor borderline region, the attack was more shallow and broad. Under identical test conditions and time of exposure, molybdenum showed no evidence of corrosion by lithium throughout the container. Metallographic examination revealed some oxidation on the outer surfaces of both materials. Determination of nitrogen content of the lithium is now is progress.

The quartz capsule that contained the metal-lithium assemblies was partially collapsed after termination of the tests at 1100°C. The collapse of the quartz container indicates the present technique has reached its maximum temperature limit. The oxidation of the outer surface of metal capsules implies that a minor leak may have developed during the test. A more reliable high-temperature vacuum system is required for future evaluations. A suitable system has been ordered and is in process of manufacture.

D. Other Reactor Fuels and Materials Development

1. Nondestructive Testing

a. Development of a Neutron-image Intensification System. An 8-Mc-bandwidth, closed-circuit television system has been placed in operation with the neutron-image intensifier. Plans are under way to replace the present f/1.4 lens on the vidicon camera in order to improve the optical system to about f/1.0. This should improve the response of the system to lower neutron intensities.

The characteristics of the present system have been studied more thoroughly in regard to contrast sensitivity and speed of response. Contrast-sensitivity values as low as 4% have been observed for steel and uranium in a narrow thickness range centered at about a two half-value-layer thickness for each material. For uranium, this thickness is about 2.5 cm, for steel about 1.9 cm. Thickness changes better than 8% can be observed for a reasonable range of material thicknesses.

Speed of response has been studied by observing the image of a cadmium arm rotating in the neutron-imaging beam. The neutron image of a $1\frac{1}{2}$-mm-diameter hole in the cadmium has been observed through the television system. Linear velocities of this cadmium object as high as 5 m/min have been observed to produce little or no blurr of the image. Linear velocities as high as 20 m/min appear to yield only minimum image blurring.

Plans are now being made to use the neutron television system for a postirradiation annealing study of an irradiated fuel sample.

E. Engineering Development

1. Development of Manipulators for Handling Radioactive Materials

a. Electric Master-Slave Manipulator Mark E4. Design, fabrication, and testing of components and subassemblies for this 50-lb-capacity manipulator have continued. Detailed layouts are in progress for the shoulder and elbow joints, and some detailed drawings of parts for these joints have been completed.

The Electric Master-Slave Manipulator Mark E4 is being designed to have the following advantages over the existing Model E3:

(i) The slave arms are arranged to do work on a vertical wall, as well as over tables or towards a ceiling.

(ii) The manipulator will be capable of operating with unshielded cables up to 500 ft long between master and slave. Cables up to about 2000 ft long can be used, but the additional length would have to be shielded. In either case, the connecting cable will have fewer conductors.

(iii) The servo amplifiers are transistorized and, consequently, are safer, since high voltages are not required.

(iv) The slave arms will be better able to work around large machinery, and viewing of the work being done will be obscured less by the arms.

(v) In addition, the Mark E4 should be more reliable, have better performance and be easier to repair.

The configuration described in Progress Report for October 1964, ANL-6965, pp. 65-66, has been mocked up completely, including pulleys, cables, and drums. The effective size of the arm between the package of servo drive units and the shoulder joint of the slave arm got to be nearly as large as a design with the servo drive units arranged in a relatively compact line grouping fairly close to the shoulder joint. This new design configuration has been mocked up and it seems to have several improvements. The design is more compact, will have less friction in the servo to arm drive linkages, will have stiffer mechanical coupling, and should be easier to repair. The X, Y, and Z motions can be directly geared instead of using a combination of gears and cables. Detail layouts of the gearing for these motions are underway

There are two possible versions of this latest design arrangement. One has the servo units in line, and the other has the servo units stacked three high to make the system shorter. Either configuration could be manufactured by using different support frames. This should give some added flexibility in the use of the slave arms for different physical requirements in different hot cells. The design of both versions is such that the cooling air or gas to be forced over the motors will come from approximately the same location as the earlier arrangements (or possibly even further from the manipulator working arms).

The master arm of the Mark E4 will be similar to the slave arm, but with tapes rather than cables to reduce friction. Since relatively straight runs are needed for tapes, the configuration must be different than that of the slave. A new system was developed to accommodate the tape runs and the required configuration.

One entire amplifier console has been completely assembled and partially tested. Some work has also been done on the assembly and testing of components for a second console. Preliminary tests indicate

that, at an ambient temperature of 115°F, the console can continuously handle adequate power for the manipulator and retain an expected component life upwards of 10,000 hr. Studies are being made to determine the possibility and practicality of operating in higher ambient temperatures.

In applications where cables longer than about 200 ft are required between the master and slave arms, some means is needed to reduce the output impedance and increase the current capacity of the position transducers and tachometers. To do this, a vacuum-tube feedback amplifier has been designed to supply reactive current to the cable connecting master and slave.

Fourteen servo drive units have also been assembled complete with synchros. Additional gears and boxes are currently being ordered so that a total of 32 units (enough for one complete pair of arms plus spares) can be assembled.

2. Two-phase Flow Studies

a. Void-fraction - Pressure-drop Facility. This experimental facility is designed to investigate the two-phase flow characteristics of boiling sodium; in particular, it is desired to obtain experimental information pertinent to the vapor volume fraction and two-phase frictional losses in an adiabatic test section.

An additional 700 hr of operation at temperatures above 1180°F have been obtained, including a maximum boiling temperature of 1600°F. In terms of void-fraction variation, boiling has been increasingly stable at higher pressure, temperature, and boiler power density. Pressure-drop and vapor-volume-fraction data have been collected, but not yet analyzed. It is planned to collect as much data as possible in a short period of time because of the inherent short operating life of the loop at the above temperatures. Future repeatability of these experiments is obviously dependent upon this lifetime factor.

3. Boiling Liquid Metal Technology

a. Niobium-1% Zirconium Loop. This facility is designed to investigate the heat transfer and two-phase flow characteristics of boiling sodium to a temperature of 2100°F and a pressure of approximately 8 atm. Among the variables to be investigated are boiling heat flux occurrence, boiling and adiabatic two-phase pressure drop, vapor volume fraction, boiling stability, and possibly flow patterns.

The construction schedule for the Nb-1% Zr loop is proceeding as planned. Pratt & Whitney reports that the material for the boiler section

has been obtained, and the first extrusion will be made shortly to determine the feasibility of fabricating the section without the difficult drilling involved in the initial design conception. The tubing order will be filled within the next 4 to 8 weeks.

Materials procurement and construction of the loop-support structure has been initiated. Discussions with suppliers concerning the forming of thin-gauge tantalum foil and the resultant structural integrity at high temperature have not yet produced sufficient information to warrant a final decision on the shutter design. An experimental shutter of thin, corrugated tantalum foil has been designed and will be fabricated to determine the feasibility of using 0.002-in. material for the remaining shutters required.

Procurement of materials for fabrication of the preheater, main heater, and loop insulation has been initiated by Central Shops.

Electrical-service installation for the vacuum chamber operation is essentially complete. Work is in progress on the bell-jar cooling circuits and instrumentation.

Instrumentation design, procurement, and calibration facilities are in progress. The differential pressure transducers have been designed and diaphragms are being fabricated. The absolute gauges, together with the constant-temperature oven for the transducer housing, are being designed.

Niobium sheath will be used with all thermocouples. Similarly, niobium instead of tantalum clamps will be used in contact with the loop tubing. Thermocouple-calibration facilities, including a high-temperature vacuum furnace, are under design and partial construction.

Reliable bucking voltage supplies for use with thermocouple outputs or recorder zero levels are being constructed by the Electronics Division.

b. Heater Experiments

(i) Thermal Radiation Heater Experiment. The purpose of the thermal-radiation-heated NaK loop is (a) to investigate thermal radiation as a means of transfering heat to and from a flowing liquid-metal loop, (b) to test some of the hardware associated with liquid-metal experiments, and (c) to observe the behavior of a liquid-metal flow loop. The thermal radiation heater has now operated for 750 hr at temperatures up to 1300°F, with heat fluxes to 62,000 Btu/hr-ft^2, and flow rates to 416 lb_m/hr. The operation of all loop components has been satisfactory. Single-phase

heat-transfer information was obtained in the laminar, transitional, and turbulent flow regions. These data appear to be in fair agreement with the semiempirical correlations of Lyon[15] and Dwyer.[16]

Boiling has occurred during 200 of the 750 hr of thermal radiation heater operation. Observations of boiling at low pressures (less than 10 psia) have shown that the initiation of nucleate boiling is accompanied by flow instabilities, an occurrence also observed by others.

Fabrication of the thermal radiation boiler and the thermal radiation preheat sections for use with the Nb-1% Zr loop are underway. Experience gained from operation of the thermal radiation heated NaK loop contributed to the design of these sections.

(ii) Electron Bombardment Heater. The basic purpose of this experiment is to investigate experimentally electron bombardment heating as a means of supplying high heat fluxes to high-temperature liquid-metal systems. It is also expected that basic information concerning pool boiling from a cylinder may be obtained.

The leaks in the electron-bombardment-heated sodium boiler have been eliminated, the surrounding clamshell heaters and insulation have been replaced, and the system has been filled with sodium. Upon completing modification of some of the system instrumentation and the fencing in of the high-voltage regions of the apparatus, the system will be ready for operation.

4. General Heat Transfer

a. Heat Transfer in Double-pipe Heat Exchangers

(i) Liquid Metal Cocurrent Turbulent Flow. Fabrication of the nickel test sections was completed. Tests will begin with the shorter test section, which has a heat-transfer length of 10 diameters and an annular ratio of 0.508. The test section will be copper plated just prior to installation in the loop; copper plating promotes surface wetting of the test fixture by mercury. However, the copper plate is soon removed, leaving a wetted nickel surface. Experience has indicated that once nickel is wetted, it will remain wetted as long as in contact with clean mercury.

Both overall and fully developed heat-transfer coefficients will be measured as a function of the weight flow rates in the tube and

[15] Lyon, R. N., Liquid Metals Handbook, 3rd ed., (USAEC and Dept. of the Navy) Washington, D. C. (1952).

[16] Dwyer, O. E., Eddy Transport in Liquid-Metal Heat Transfer, AIChE Journal, 9(2) (March 1963).

annulus. The results will be correlated in terms of the four basic dimensionless parameters (see Progress Report for June 1964, ANL-6912, p. 72).

Prior to the fitting of the test sections to the loop, a preliminary heat balance was made to check out the instrument calibrations. The loop was not insulated, since the nickel test sections were not completed at the time. Deviations of 4% across the water cooler, 7% across the heater, and 12% across the stainless steel test section were obtained. It is expected that these results will be greatly improved when the loop is insulated.

5. ANL-AMU Program

Other heat engineering experiments, performed as part of a joint program between the Laboratory and the Associated Midwest Universities (AMU), are described below.

a. Inception of Hydrodynamic Instability in a Natural-circulation Boiling Loop. Some of the observations from experiments completed with two sets of loop geometry: (1) 96-in.-long, 0.8125-in.-ID test section with a 50-in.-long, 1.049-in.-ID riser, and (2) 96-in.-long, 0.364-in.-ID test section with a 50-in.-long, 0.3125-in.-ID riser are discussed here.

In the literature, the data on the threshold of hydrodynamic instability is reported in numerous ways, for example:

(a) the heat flux at which ±10% variation in the pressure drop across test section takes place;[17]

(b) the heat flux at which random oscillations in the pressure drop across the venturi begin;[18]

(c) the root-mean-square value of the inlet flow-rate signal at the instability frequency (obtained from the power-density spectrum) plotted against heat-flux.[19]

---

[17] Levy, S., and Beckjord, E. S., Hydraulic Instability in a Natural Circulation Loop with Net Steam Generation at 100 psia, GEAP-3215 (July 1959).

[18] Anderson, R. P., and Lottes, P. A., Boiling Stability, Progress in Nuclear Energy, Series IV, 4 (1961).

[19] Spigt, C. L., et al., The Onset of Hydraulic Instabilities in an Annular Channel, Technological Univ. of Eindhoven, Report No. WW016-R53.

Each of the above methods was used for the analysis of a few sets of experiments. The amplitude of oscillation of pressure drop across the test section or Venturi is dependent on the system pressure and inlet subcooling, and under certain conditions, the system is unstable even though the oscillations are less than ±10%. Thus, the arbitary ±10% criterion of instability is unsatisfactory for a complete range of system pressure (200-1500 psia) and inlet subcoolings (0-50°F). The procedure for obtaining the plots similar to the Eindhoven work[19] is complicated and necessitates the use of modern electronic devices, such as an FM tape recorder, an analog to digital converter, and a digital computer, for a quick and accurate analysis. Moreover, this correlation work is unnecessary for the present work, since the information from the differential pressure transducers and thermocouples is more or less periodic in character, with no tendency to converge or diverge, except at the burnout point. On analysis, the high-frequency oscillation component (frequency more than 1 c/s) in these signals was found to be caused by the natural frequency of the transducers and noise pickup by the recording instruments. These were eliminated to a great extent by suitable filtering devices taking care that the actual information was not cut-off.

Plots of standard deviation of pressure drop across the Venturi, inlet flow rate and pressure drop across test section and riser against heat flux (see Figure 13) indicate the spread of data at a given power level. The curve profiles are similar to those obtained at Eindhoven University and also similar to the plot of temperature difference between wall and bulk fluid in the test section plotted against heat-flux. These plots clearly indicate that there is no sharp change in the system behavior at some heat flux for given conditions; thus, the threshold point cannot be pinpointed without some arbitrary definition.

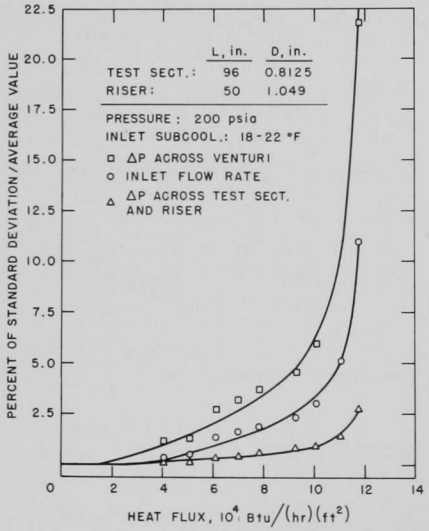

Figure 13. Data Scatter vs. Heat Flux

A digital computer program (STABLE-3, CDC-3600 computer; see Progress Report for October 1964, ANL-6965, p. 71) was completed, based on the closed-loop transfer-function analysis of linearized equations developed by Jones.[20] In this work, Nyquist criterion is used for the prediction of instability. In Figure 14,

[20] Jones, A. B., Hydrodynamic Stability of a Boiling Channel, KAPL-2170 (Oct 1961).

two Nyquist plots, calculated for the same input conditions as for the data in Figure 13, are shown. The point of inception of instability is predicted to be approximately 1.05×10^5 Btu/hr-ft^2 for the stated conditions.

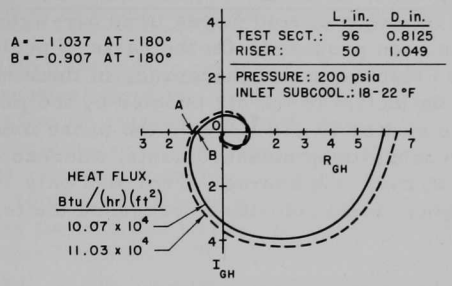

Figure 14. Nyquist Plot as Obtained from Jones Model

The actual system is nonlinear, and the experimental observations point without any doubt to sustained hydrodynamic oscillations, or oscillations around an extremely weak focus. The envelope of these oscillations increases with increasing heat flux. It is, therefore, quite easy to see that the analyses such as above, and other existing linear and nonlinear solutions of the system, are incomplete. These analyses consider whether the dependent variables tend towards the equilibrium point or diverge away when some disturbance is introduced (infinitely small disturbance in case of linearized analyses); in the former case the system is predicted to be stable and unstable in the latter. The analyses, however, do not consider whether these so-called unstable trajectories diverge to infinitely or converge on to a "limit cycle." A realistic solution should lead to these "limit cycles," so that the analysis may match with the actual experimental observations. An attempt is being made in this direction.

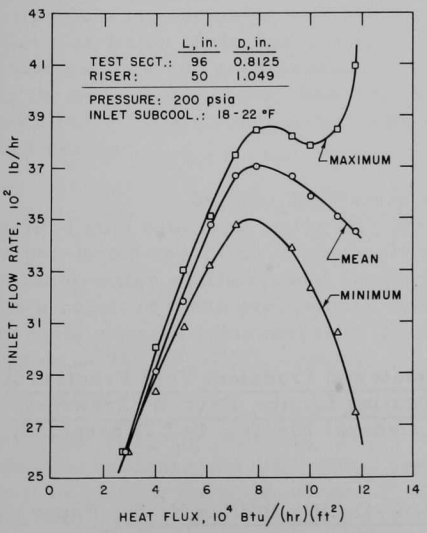

Figure 15. Peak and Mean Values of Inlet Flow Rate vs. Heat Flux

On the basis of the above discussion, the analysis of data should consist of the plots of mean values of the signals and the envelopes of the maximum and minimum values at different power levels. A set of typical plots is shown in Figure 15, for inlet flow rate. Such plots supplemented by the values of the

frequency of oscillation give complete information about the system behavior at different power levels for a given set of parameters.

b. Propagation of Void Waves in an Air-Water System. In the investigation of the behavior of void waves in an air-water system, an electrical probe has been proposed. On the basis of preliminary experiments, it is believed that the major inaccuracy of the electrical resistivity probe is due to the deflection of the air bubbles by the probe itself. At low superficial liquid velocities (0-1.0 ft/sec), the probe measurements were about 35% below pressure-drop measurements, whereas at higher liquid velocities (1.0-4.0 ft/sec), the average error was only 7%. This tends to indicate that the higher liquid velocities decreased the tendency of deflection.

The probe response for void-wave tests was analyzed for five different axial positions and five different radial positions at each set of operation conditions. The first six sets of conditions were with a zero steady-state void fraction and the perturbation void fraction varied from 3% to 15%. The data indicated that the propagation velocity of the perturbations was accurately predicted by steady-state data. These results agreed with those of Zuber[21] and, at the same time, could be predicted by the bubble rise velocity equation:

$$V_b = K_1 K_3 \sqrt{g D_b} + K_2 \left(\frac{Q_f + Q_g}{A} \right)$$

given by Griffith.[22]

---

[21] Zuber, N., and Hench, J., Steady-state and Transient Void Fraction of Bubbling Systems and Their Operating Limits, Part II: Transient Response, Report No. 62GL111, General Electric Co., Schenectady, N. Y. (July 1962).

[22] Griffith, P., The Prediction of Low-Quality Boiling Voids, Paper No. 63-HT-20, Meeting of ASME in 1963, appearing in J. Heat Transfer.

F. Chemical Separations

1. Fluoride Volatility Processes

a. Recovery of Uranium from Low-enrichment Ceramic Fuels

(i) Laboratory Support Work. Laboratory work in support of the pilot-plant investigation of the fluid-bed fluoride volatility process has continued. Separation of uranium and plutonium from fission product elements occurs mainly during the fluorination step wherein volatile UF_6 and PuF_6 are removed from the reactor and nonvolatile fission product fluorides remain associated with the alumina fluid-bed material. It is planned to use the alumina bed for several processing cycles (see Progress Report for November 1964, ANL-6977, p. 67). This processing scheme would result in the continued accumulation of fission products in the alumina bed. Therefore, a study has been made to determine the manner in which the fission products are distributed in the fluid-bed material.

The alumina bed and disengaging chamber residue from a test which involved the fluorination of PuF_4, UO_2F_2, fission product fluorides, and iron oxides (see ANL-6977, p. 67) was used as a source material for analysis of fission product distribution. Zirconium was chosen as the typical fission product. Screen analyses of the material indicated that 1% of the material was -230 mesh. Analyses of the materials indicated that, although the zirconium concentration in the fines fraction (-230 mesh) was greater than in the coarse fraction, a major portion of the zirconium is associated with the coarser material. These data suggest that elutriation of the fine particles from the alumina bed material after fluorination would not significantly reduce the fission product concentration in the bed. This subject, however, will be studied further in tests performed with PuO_2-UO_2-fission product feed materials in the 2-in.-diameter fluid-bed reactor.

In other laboratory work a study of the vapor-liquid and solid-liquid equilibria in the UF_6-PuF_6 system is being conducted. The vapor-liquid apparatus is currently being tested by determining the ethanol-water equilibria and comparing the data with published values. As a result of these preliminary determinations, it has been necessary to make several adjustments in the equipment before attempting measurements on the UF_6-PuF_6 system.

Initial tests in the solid-liquid apparatus were performed with the MoF_6-UF_6 system. These tests were made using the techniques of thermal analysis and differential thermal analysis, since these techniques will be used in the study of the UF_6-PuF_6 system. Preliminary results on the MoF_6-UF_6 system indicate that a simple eutectic exists at 14°C and 87 m/o MoF_6.

(ii) Decladding and Fluorination Experiments with Uranium Dioxide Fuels. Development work in support of the fluoride volatility pilot plant is continuing in fluid-bed equipment to establish optimum processing conditions for the decladding and fluorination steps employed in reprocessing ceramic UO_2 fuels. Processing studies using feed materials of uranium only are being conducted in a $1\frac{1}{2}$-in. dia. bench-scale reactor and in a 3-in. dia. pilot-scale reactor. Tests with plutonium-containing fuel are being made in a 2-in. dia. fluid-bed reactor. Zircaloy-clad or stainless steel-clad UO_2 fuel elements are chemically declad by the high temperature reaction of the cladding with a gaseous mixture of HF-O_2 (see Progress Report for September 1964, ANL-6944, pp. 69-70). During the decladding step, the oxide fuel reacts with the decladding agent to form a powdered mixture of UO_2F_2 and UF_4. This material is then fluorinated with fluorine gas to recover uranium (and plutonium) as the volatile hexafluoride.

Development work with uranium feed materials in a 3-in.-diameter reactor is primarily directed toward establishing optimum processing conditions for fluorinating mixtures of UO_2F_2 and UF_4. Current work has concerned itself with the modification of instrumentation of the process equipment. Included in these modifications was the installation of a facility for producing γ-ray radiographs which will be used to observe the UO_2 pellets during the decladding and fluorination steps.

To facilitate selection of decladding conditions for pilot-scale runs in the 3-in.-diameter reactor with Zircaloy-clad UO_2 fuel, two tests were made in the $1\frac{1}{2}$-in.-diameter bench-scale reactor to demonstrate the destructive oxidation of Zircaloy with a gaseous mixture of HF and O_2. In a test in which a solid rod of Zircaloy-2 was suspended in a fluid-bed of alumina and contacted with a gaseous mixture of 40 v/o HF-40 v/o O_2-20 v/o N_2 for 3 hr at 550°C, an average penetration rate of 15 mils/hr was observed. Similar penetration rates for Zircaloy cladding were observed in the second test in which Zircaloy-clad UO_2 pellets were reacted with the same gaseous mixture for 3 hr at 550°C. Most of the UO_2 pellets were pulverized by reaction with HF-O_2 during the 3-hr reaction period; only 11% of the UO_2 charge remained intact as clad pellets at the end of the test. The results of these tests have provided the information needed for the selection of processing conditions for studies in the 3-in.-diameter reactor.

In preparation for tests with plutonium-containing feed material, several runs are being performed in the 2-in.-diameter fluid-bed reactor with UO_2 fuel. In recent work an alternative method for reprocessing ceramic oxide fuels was investigated. This method involves the fluorination of a packed bed of sintered UO_2 by the two-zone oxidation fluorination procedure (see Progress Report for October 1963, ANL-6801, pp. 60-61). In the oxidation-fluorination processing scheme, the lower (oxidation) zone of the reactor consists of a bed of declad, sintered

UO_2 pellets with sintered alumina particles filling the voids of the bed, and the upper (fluorination) zone consists of a fluidized bed of sintered alumina particles. Passing an oxygen-nitrogen stream through the lower zone causes U_3O_8 fines to be produced and transported to the upper fluidization zone, where the fines are fluorinated to UF_6. In this test a 2-in.-deep bed of sintered UO_2 pellets was immersed in an 11-in.-deep bed of -48 +100 mesh alumina particles. The oxygen concentration in the fluidizing gas stream was 18 v/o. The fluorine feed in the side inlet above the pellet bed was diluted with 50 v/o nitrogen, which gave a fluorine concentration in the fluid bed of 7 v/o. The two-zone oxidation-fluorination step was conducted for 3 hr at 500°C. This was followed by an extended recycle-fluorination period (5 hr at 500°C, followed by 10 hr at 550°C) in which the entire bed was fluorinated with 80-95 v/o fluorine. This fluorination procedure was adopted to simulate the procedure employed in the fluorination of plutonium feed materials (see Progress Report for September 1964, ANL-6944, pp. 68-69).

A total of 99.9% of the uranium was recovered as UF_6 in the cold traps and NaF traps. The uranium concentration on the alumina bed at the end of the run was 0.014 w/o. Fluorine efficiency during two-zone operation was approximately 60%. No processing difficulties were experienced during the test. It was observed that fines buildup in the disengaging and filter sections of the reactor was greatly reduced in this test as compared to tests in which UO_2 pellets were pulverized with $HF-O_2$ mixtures (see Progress Report for December 1964, ANL-6997, pp. 40-41).

(iii) Engineering-scale Alpha Facility. An engineering-scale alpha facility (see Progress Report for November 1964, ANL-6977, p. 68) is being installed to permit demonstration of the major steps of the fluid-bed fluoride volatility process for the recovery of uranium and plutonium from ceramic oxide fuels. Equipment units for processing batches of UO_2-PuO_2 pellets to hexafluorides and for demonstrating the conversion of hexafluorides to oxides are nearly completely installed in the facility. The conversion unit will also be used to demonstrate the separation of plutonium (as PuF_4) from a mixed uranium-plutonium hexafluoride feed by thermal decomposition. A distillation unit for purifying and separating UF_6 and UF_6-PuF_6 product streams is being designed for the alpha facility.

Tests which are planned for the fluorination equipment involve the use of $HF-O_2$ mixtures for pulverizing unclad UO_2 pellets. A hydrogen fluoride supply and metering system has been installed in the facility. The system consists basically of a 25-lb cylinder of HF in a constant-temperature water bath which is located in a ventilated enclosure in the main cell area. The supply tank and bath are mounted on a scale, which, in addition to the use of a rotameter, provide the means for metering the HF flow rate. Upon completion of work projects involving the insulation of process lines and the calibration of several process instruments, shakedown tests with uranium materials will be resumed.

All major construction and installation work on the hexafluoride-to-oxide converter has been completed. Current activity consists of checkout of operational systems, effecting minor equipment modifications, and insulating the reactor and all heated process lines.

b. Recovery of Uranium from High-enrichment Fuels

(i) Pilot-plant Demonstrated Runs. The final series of pilot-plant experiments has been completed in which the recovery of uranium from highly enriched uranium alloy fuels by the fluid-bed, fluoride volatility process was demonstrated. During this program, a total of 18 runs were made wherein 24 fuel elements were processed. Results of recent runs were published previously (see Progress Report for December 1964, ANL-6997, pp. 41-45).

The major tasks remaining in the pilot-plant program concern the inspection and evaluation of the pilot-plant equipment and instrumentation, and correlating corrosion data obtained during the course of the 18 runs.

(ii) Processing of Uranium Dioxide-Stainless Steel Cermet Fuel. Bench-scale development studies on the decladding and fluorination of UO_2-stainless steel cermet fuels clad with stainless steel were continued. The process employs two principal steps: (1) a decladding step in which chemical destruction of the stainless steel cladding and fuel matrix is accomplished by oxidation with gaseous mixtures of HF and O_2; and (2) a fluorination step in which uranium is recovered as UF_6 by reaction of the fuel material with fluorine.

A demonstration test was performed in a $1\frac{1}{2}$-in.-diameter fluid-bed reactor using a 90-g fuel-element charge. The processing conditions for this test were essentially the same as for the test reported previously (see Progress Report for November 1964, ANL-6977, p. 69). Decladding was conducted at 550°C with a gaseous mixture of 40 v/o HF, 40 v/o O_2, and 20 v/o N_2. A three-step fluorination procedure was employed: 3.3 hr at 250°C while the fluorine concentration in the feed gas was increased from 5 to 90 v/o; 4 hr with 90 v/o F_2 in nitrogen while the bed temperature was increased from 250 to 550°C; and 1.0 hr at 550°C using 95 v/o F_2. The total fluorination period was 8.3 hr.

High uranium recovery (>99%) was indicated by the low uranium concentration in the alumina bed material after fluorination (0.005 w/o uranium). The quantity of uranium retained on the alumina was equivalent to 0.2 w/o of the uranium in the cermet fuel charge. These results, when compared with those from a previous test in which the total fluorination period was 11 hr (ANL-6977, p. 69), indicate that high uranium recoveries can be achieved in an 8-hr fluorination period and that extended fluorination does not result in increased uranium recovery.

2. General Chemistry and Chemical Engineering

a. Determination of the Critical Constants of Alkali Metals. Studies to determine the critical constants of alkali metals (see Progress Report for November 1964, ANL-6977, pp. 70-71) have been continued. Current work is on rubidium and cesium. Densities of the vapor and liquid phases of rubidium (containing radioactive ^{86}Rb) are being measured from room temperature up to the critical point by measurement of gamma radiation emanating from the vapor and liquid regions of rubidium held in a small capsule. As the critical point is approached, the densities of the vapor and liquid, and therefore the gamma activities emanating from the vapor and liquid regions, approach each other. The vapor and liquid densities of rubidium have been measured to 1720°C. Based on these data, it is estimated that the critical temperature is between 1770 and 1870°C, and that the critical density is between 0.33 and 0.37 g/cc. This temperature is well below on Grosse's estimate[23] of the critical temperature, 1917°C, but agrees with his estimate of critical density, 0.32 g/cc, and is well above Hochman and Bonilla's estimate[24] of 1727°C for the critical temperature.

By use of the same technique, additional runs have been made for the determination of the critical constants of cesium. The estimated critical temperature, based on data to 1635°C, is between 1800 and 1900°C, and the estimated critical density is between 0.38 and 0.42 g/cc. These are close to von Grosse's estimates[23] of 1887°C and 0.42 g/cc, but considerably above the critical temperature of 1783°C obtained by Hochman and Bonilla. Additional runs will be made with rubidium and cesium to replicate the results and to approach the critical points more closely.

b. Calorimetry. Recent improvements in metal-combustion techniques for fluorine bomb calorimetry have led to a redetermination of the standard enthalpy of formation of aluminum trifluoride, AlF_3 (see Progress Report for July 1962, ANL-6597, p. 45). Significant improvement in the results was obtained by the following experimental modifications:

(a) Difficulties of ignition and of insufficient burning were overcome by eliminating the (AlF_3) sample dish and cover arrangement. Instead, 5-mil aluminum foil was formed into a small basket into which aluminum filings were placed. The sample was ignited by a cadmium fuse wire while suspended by a fine aluminum wire from a heavily fluorinated

---

[23] von Grosse, A., The Liquid Range of Metals and Some of their Physical Properties, NP-10795 (Sept. 5, 1960).

[24] Hochman, J. M., and Bonilla, C. F., The Electrical and Thermal Conductivity of Liquid Rubidium to 2900°F, J. Electrochem. Soc. 111, 200C (Aug 1964). Also Extended Abstracts of Electrothermics and Metallurgy Division, The Electrochemical Society, Inc., Fall Meeting, Washington, D. C., Oct. 11-15, 1964, 2, No. 2, p. 58.

[25] Hochman, J. M., and Bonilla, C. F., The Electrical and Thermal Conductivity of Liquid Cesium to 3000°F and the Critical Point of Cesium, Trans. Am. Nucl. Soc. 1, 101 (June 1964).

nickel post. With this arrangement, the sample became sufficiently hot so that when it dropped to the bottom of the calorimeter bomb, quenching of the reaction was considerably reduced.

(b) The interior surfaces of the bomb were protected from sputtering metal by a liner of tamped, purified AlF_3 which had been pre-fluorinated with a gaseous $HF-ClF_3$ mixture.

(c) Determination of the unreacted aluminum, which was usually in the form of beads, was improved by rolling the beads into foils, thereby enabling them to dissolve more readily in acid.

With the use of these modifications, a series of nine aluminum combustions yielded the value $\Delta Hf^{\circ}_{298}(AlF_3, c) = -361.1 \pm 0.6$ kcal mole^{-1}. (The quoted uncertainty is double the overall standard deviation of the mean.) This value agrees favorably with values previously reported in the literature (see table below) which were obtained by both direct[26,27] and indirect[28-30] methods.

	$\Delta Hf^{\circ}_{298}(AlF_3, c)$, kcal mole^{-1}
This work	-361.1 ± 0.6
Domalski[26]	-360.4 ± 1.6
Domalski[27]	-358.5
Gross et al.[28]	-358.6
Kolesov et al.[29]	-357.7
Mashovets and Yudin[30]	-357.3

G. Plutonium Recycle Reactors

1. Physics Calculations

Various partial plutonium loadings will be examined experimentally in the EBWR in the initial approach to the 36 plutonium-element zoned-critical configuration.

---

[26] Domalski, E. S., private communication (1964).

[27] Domalski, E. S., NBS Report 7587, U. S. Department of Commerce (July 1962).

[28] Gross, P., Hayman, C., and Levi, D. L., Bull. of Chem. Thermodynamics 2, 21 (1959).

[29] Kolesov, V. P., Martyuov, A. M., and Skuratov, S. M., Russian Journal of Inorg. Chem. 6, 1326 (1961).

[30] Mashovets, V. P., and Yudin, B. F., Tsvetnaya Metallurgiya 4, 95 (1962).

Since the central control rod worth is enhanced with partial loadings, a study was made of the rod withdrawal incident for various partially loaded plutonium zone configurations. In a previous safety analysis study, it was concluded that a rod withdrawal incident does not lead to a serious excursion for the fully loaded system.

a. Rod Worth Results. PDQ-3 calculations were made for the initial plutonium zone configuration having 16 and 24 elements. Table XVII presents the results for the central rod worths, remaining 8-rod worths, and total 9-rod worths, together with the previously obtained results for the full 36-element plutonium zone.

Table XVII. Rod Worths with Various Plutonium Zone Sizes

Number of Elements	Central Rod Worth, Other Rods In	8-rod Worth, Central Rod Out	9-rod Worth
16	0.137	0.023	0.160
24	0.120	0.046	0.167
36	0.097	0.062	0.159

Taking the active rod length as 48 in. and the maximum central rod speed as 4.3 in./min, the maximum rate of reactivity change for the 16-, 24-, and 36-element cases are respectively 13.3, 11.7, and 9.4 cents/sec. This assumes $\beta = 0.00307$ and that the maximum insertion rate is twice the average insertion rate.

The unpoisoned critical loading for the plutonium zone is calculated to be 17.7 elements.

b. Ramp Incident Results. RP-129 J calculations were made for two cases of possible ramp incidents. Case I describes an incident where Doppler feedback corresponds to a 17.7-element loading and a linear insertion rate based on a 16-element rod worth; since rod worth varies inversely with the number of fuel elements, this assumption provides some margin of conservatism. Case II describes an incident where the Doppler feedback and insertion rate corresponds to the 36-element loading. It should be pointed out that no credit was taken for the loss of reactivity due to heat transfer to the water.

The results from the solutions of these two problems are presented in Table XVIII. The reactor is assumed to be critical and at 1 W when the ramp test is initiated.

Table XVIII. Ramp Insertion Results

Doppler Shutdown Corresponding to	Insertion Rate Corresponding to	Time to Reach Infinite Period (sec)	Minimum Period (sec)	Maximum Power (MW)	Integrated Power at 20 sec (MW-sec)
17.7 Elements	16 Elements	8.7	0.10	29	68
36 Elements	36 Elements	11.7	0.12	25	58

The integrated powers required to reach melting at the hottest spot in the core are respectively 181 and 390 MW-sec for the two cases shown in Table XVIII. These numbers can be compared with the integrated powers at 20 sec given in Table XVIII. These integrated powers would correspond to the wholly unrealistic case of continued withdrawal for 20 sec at the maximum rate, and as mentioned earlier would take no credit for heat transfer to the water.

The results presented here clearly indicate that the control rod withdrawal incident in EBWR is not of major consequence.

c. Resonance Capture. A formula for estimating the mean chord length of a fuel lump (see Progress Report for October 1964, ANL-6965, pp. 47-48) has been modified. The original equations are

$$\int_0^\infty \frac{dE}{E}\,\sigma_a\left(\frac{1}{\ell}-\frac{1}{\ell_e}\right)\frac{\Sigma_t-\Sigma_p}{[(1/\ell_e)+\Sigma_t]^2} = 0 \qquad (1)$$

has been changed to

$$\int_0^\infty \frac{dE}{E}\,\sigma_a\left(\frac{1}{\ell}-\frac{1}{\ell_e}\right)\frac{(\Sigma_t-\Sigma_p)^2}{[(1/\ell_e)+\Sigma_t]^3}\,\frac{1}{[(1/\ell)+\Sigma_p]} = 0. \qquad (2)$$

Based upon numerical analysis, it appears that Eq. (1) underestimates the effective mean chord length, ℓ_e, whereas Eq. (2) overestimates it.

d. Total Neutron Cross Sections. A Fortran code for the CDC-3600 has been written which calculates both single-level and multilevel cross sections as a function of energy for purely scattering resonances such as occur in the light metals. Cross sections are calculated with use of the natural line shape where orbital angular momentum values of $\ell = 0, 1,$ and 2 are allowed. Calculation of a background cross section produced by distant resonances is optional in the multilevel code.

2. Fuel Development and Fabrication

Further evaluations of the PuO_2-UO_2 fuel rods for the central zone which contained transverse cracks in the tube wall or body of the lower end

plug were completed at Hanford (see Progress Report for December 1964, ANL-6997, p. 49). These cracks were the result of uncontrolled harmonic vibrations normal to the vertical axis occurring during vibratory compaction of the fuel.

Thermal-cycling tests at Hanford indicated that defects of this type as small in 51 μ in depth could propagate. Not all observed defects were found to propagate, and the number of cycles introduced by the test exceeded what would normally be expected during the length of the Plutonium Recycle Experiment. Even though failures might not occur in the reactor, considering the relative ease with which the rods could be reworked at this time, it was agreed that all fuel rods at ANL would be reinspected and reworked as required. All fuel rods at ANL, including those already assembled into fuel elements were returned to Hanford.

A total of approximately 624 reworked PuO_2-UO_2 fuel rods have been returned from Hanford. This is sufficient to load a total of 17 fuel elements for the reactor critical loading of the unpoisoned plutonium-zone fuel when the control rods are withdrawn from the core.

A total of 30 Zircaloy-2 fuel cans for the central-type plutonium fuel elements have been received from United Nuclear Corporation. Ultrasonic testing of 179 unloaded Zircaloy-2 tubes showed no defects. All fuel grids and end fittings have been assembled in these cans, which are now ready for insertion of the removable-type PuO_2-UO_2 fuel rods.

The fabrication of enriched shim elements containing 6% enriched UO_2 pellet-type fuel, and driver fuel elements containing normal UO_2 pellets is continuing at United Nuclear Corporation. A total of seven of the enriched shim elements are completed and will be delivered to the Laboratory as soon as shipping containers become available.

3. EBWR Facility

Combinations of ultrasonic, dye-penetrant, magnetic-particle, and radiographic inspections were utilized in the examination of piping, reactor vessel, and auxiliary equipment to assess the integrity of the facility. Field inspection (see Progress Report for December 1964, ANL-6997, pp. 47-48) is approximately 75% completed. Thus far, the inspections show that only minor changes have resulted from exposure to the operational environment. However, some poor workmanship and some intermixing of materials were also found. All imperfections discovered are repairable. Summaries of findings are as follows:

a. Vessel Closure Cover. Under test by ultrasonic probes, no evidence of defects in either thickness or radial direction in ligaments between bolt holes or in metal inscribing and circumscribing the bolt hole

plane was found. Sonic examination augmented by a Magnaflux inspection of every eighth bolt hole showed no cracking at hole edges.

b. Vessel Closure. Ultrasonic probes revealed no evidence of defects in either the thickness or radial direction in the ligaments between bolt studs.

c. Vessel Closure Bolting. Magnaflux and longitudinal sonic probes of all 44 bolt studs showed that the strength members were sound.

d. Steam Piping. Sonic thickness measurements of the original 6-in. steam and safety valve line were completed. Two regions were found where the wall was below the minimum wall thickness required by the ASTM standards, but still substantially greater than the required design thickness (0.264 in. vs. 0.217 in.). A plug was removed from the wall approximately 9 in. away from one of the thin regions for visual examination and measurement. It was found that the sonic thickness measurement conservatively estimates the minimum wall: the actual found was 0.273 in.

A number of welds require repairs. Radiographs indicate that the defects are either cracks or incompletely fused adjacent passes in the multi-pass weldments.

Magnaflux examinations of welds were inconclusive; the defects were apparently too deep to be discovered by this technique.

e. Startup Heater Piping. No evidence of internal corrosion, either general or local, was found by sonic thickness measurements of the 3-in. and 4-in. stainless piping. Dye-penetrant examinations of the pipe welds and pipe exterior showed sound materials. Radiography revealed a number of welds with incompletely fused roots.

It is not now possible to judge the strength of the partially welded connections because of the scattering of the gamma radiation (Ir^{192}) by the front wall.

f. Boric Acid Injection Piping. Visual inspections revealed the utilization of Type 347 piping fittings (elbows and reducers) in a Type 304 system. Radiographs revealed poor welding workmanship - up to 50% unfused wall. Economics dictated a complete replacement in preference to repairs to the existing (and partially inaccessible) line. The line was removed and will be replaced and relocated with a substantially shorter line containing fewer welds.

g. Feedwater Filters. No. 1 and No. 2 stainless-clad carbon-steel shell filters (original units) are satisfactory but must be re-rated for maximum temperature. The necessary calculations to meet ASME Code

Requirements are in progress; the design review was made necessary by the use of 600-lb flanges on the inlet and outlet connections to the filter.

No. 3 and No. 4 all-stainless-steel filters contain numerous exterior surface cracks aligned parallel with the longitudinal axis. Each filter also contains an exterior surface plate defect, believed to be repairable by welding. These original units must also be re-rated for maximum temperature and for the same reason, that is, limitations imposed by 600-lb flanges.

h. Reactor Vessel Cladding. The steam collector duct and the two shock shield sections were removed from within the reactor vessel to establish the integrity of the resistance-welded cladding. Couplings were welded to the 7/64-in.-thick cladding for the introduction of nitrogen (under pressure) between the cladding and SA 212-B steel shell. While under pressure (100 psi min), the surface will be coated with liquid soap for the discovery of through cracks.

The upper one-third part of the wrought cladding is decorated with a random distribution of fine cracks readily visible but not indicated by dye penetrant. Two perforations of the cladding were found adjacent to manual-deposited overlays and are believed to be induced by accidental mechanical damage.

i. Containment Shell Doors. Three partially cracked structural fillet welds between the door plate and stiffener bars were found on the inner door in the Magnaflux inspection of the air lock doors. The cracks were ground out, rewelded and reinspected prior to a 2-psi test of the air lock. The air test showed that the welding operations had not affected the door frame seals. Methods of further strengthening of the door plates are under study.

III. ADVANCED SYSTEMS RESEARCH AND DEVELOPMENT

A. Argonne Advanced Research Reactor (AARR)

1. Design of the Outer Radial Reflector: Theory

In the present reference design of the outer radial reflector, local "flux-traps" are included in the form of water zones at the tips of the horizontal beam tubes. A thin (0.5 cm) region of zirconium, representing the followers of the peripheral control blades, is the first reflector zone; then beryllium, with some cooling water; then water, locally; then a thick zone of beryllium and coolant water, which is penetrated by beam tubes; and finally a water zone and shielding.

In previous calculations of reactivity and of flux distributions, the composite regions have been: 2.5 cm of beryllium with 6.8% water; 4.3 cm of water; and 24 cm of a zone comprised of 81% beryllium, 4% beam-tube metal, 3% water, and 12% void. This configuration simulates the effect of the flux-trapping near the beam tubes, which seems to be quite effective in increasing the thermal neutron flux in the vicinity of the tips of these tubes.

There would be a number of distinct advantages in engineering design, however, if the beam tubes were not required to penetrate the beryllium. The simplest way to accomplish this is to increase the thickness of the inner zone of beryllium, e.g., from 2 to 4 in., and to leave off the outer beryllium zone. Two questions of prime concern are: (1) what would be the effect on the density of thermal neutrons exiting from the beam tubes; and (2) what would be the reactivity effect of such changes in the radial reflector?

Preliminary answers to these questions are supplied in Table XIX and in Figure 16, namely, that there would be a reactivity gain, but probably with some reduction in the density of emergent thermal neutrons. The curves in Figure 16 are normalized to a constant power level, but otherwise there is no significance to their absolute magnitudes. The unnormalized results were obtained as the output of 16-group diffusion theory in cylindrical geometry using the RP-122 program (one space dimension).

Table XIX. Effective Multiplication Factors for Fresh Operating Reactor without Burnable Poison Control

Reflector Composition	k_{eff}
Reference system with flux-traps near tips of beam tubes	1.161
3-in. beryllium with 3% water; then water	1.199
3-in. beryllium with 3% water; 3-in. beryllium with 1% water; then water	1.225

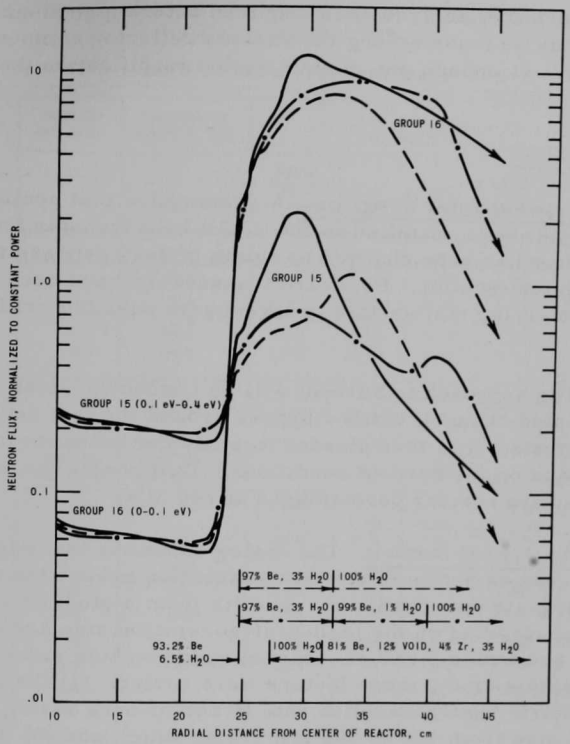

Figure 16. Distribution of Thermal-neutron Flux in Radial Reflector of AARR for Various Reflector Compositions

In Figure 16 are plotted the neutron fluxes for energy groups 15 and 16, the two "thermal" groups of the set. Three cases are shown: (1) the reference radial reflector, described above (2) a reflector with a total of 6 in. of beryllium (plus some water), without beam-tube penetrations; then water, ignoring the voids and metal of beam tubes; and (3) a reflector with 3 in. of beryllium plus 3% water; then water.

Although the radial distributions of power are not shown in Figure 16, the shapes of the thermal-neutron fluxes correspond approximately to the powers, in the sense that the radial distribution of power is flattened in the bulk of the core when the thickness of the inner zone of beryllium is increased. Therefore, for the same total power, the peak powers, at the inner and outer edges of the reactor core, are lower. With small change in the total power, a reduced grading in fuel loading would increase the leakage of high-energy neutrons from the core, and, in particular, would raise the peak flux in the reflector for the case of a 3-in.-thick beryllium annulus.

More detailed analyses are required before a good quantitative comparison may be made among the various reflector compositions of interest. There is enough potential in such a modification that such analyses will be made.

2. Heat Transfer

a. Experimental Program. A rectangular test section, 0.040 x 1.25 x 18 in., has been installed in the AARR heat transfer loop, and the burnout detector has been changed to obtain better response to prevent burnout of the test section. Pressure transducers have been installed in the exit region of the test section to investigate possible critical flow phenomena.

The approach to burnout will be conducted, first, with a single, uniformly-heated channel, with no bypass around the test section, followed with burnout tests. It is then planned to study the influence of the parallel unheated bypass on the burnout conditions. Test conditions will approximate steady-state reactor performance at 240 MW.

b. Analytical Studies. The analog computer investigation of the effect of a linear variation of the heat generation across the thickness of an AARR fuel plate was continued. Results from a study of a fuel plate with 0.004-in. cladding on the high-heat-generation side and 0.006 in. on the low side and with a 0.040-in. channel space on both sides are listed in Table XX. In this study, these factors were varied: (1) the ratio of high to low volumetric heat-generation rate (front-to-back ratio), (2) the time for power to rise from 100 to 300 MW (ramp time), and (3) the effect of the film coefficient of heat transfer. The results indicate that as the power is being raised, the heat-flux ratio reaches its first peak because of the effect of the heat transfer film coefficient and temperature gradients in the fuel. After the first peak, the ratio decreases slightly and stays above the 100-MW value until local boiling occurs on the thin cladding side. The heat-flux ratio then peaks again at a higher value, and decreases after local boiling begins on the side with the thick cladding and low heat-generation rate. The final steady-state, 300-MW ratio heat flux settles out at a value above the 100-MW heat flux ratio but below the first peak.

A second run made with this analog model corresponded to the power transient from a $0.75 step increase in reactivity. The change in the temperature of the channel coolant due to this transient was also incorporated into the simulation in which 0.040 coolant channel was used. Both of these curves are based on the PSAR analog transient study.

The 100-MW heat-flux ratio was 1.122. The first peak, second peak, and 300-MW ratios were 1.21, 1.345 and 1.155, respectively. The duration of the transient to and from the second peak was about 14 msec.

Table XX. Results of Heat-flux Ratio* Study Using the Ramp Power Profile

CASE 1: EFFECT OF FRONT-TO-BACK RATIO

FRONT-TO-BACK RATIO	POWER PROFILE RAMP RISE TIME	HEAT-FLUX RATIO			
		STEADY STATE AT 100 MW	FIRST PEAK	SECOND PEAK	STEADY STATE AT 300 MW
—	msec	—	—	—	—
1.0	12.5	1.085	1.125	1.170	1.095
1.15	12.5	1.115	1.170	1.220	1.140
1.0	100.0	1.080	1.100	1.170	1.100
1.15	100.0	1.115	1.140	1.225	1.140

CASE 2: EFFECT OF RAMP RISE TIME

FRONT-TO-BACK RATIO	POWER PROFILE RAMP RISE TIME	HEAT-FLUX RATIO			
		STEADY STATE AT 100 MW	FIRST PEAK	SECOND PEAK	STEADY STATE AT 300 MW
—	msec	—	—	—	—
1.00	12.5	1.085	1.125	1.170	1.095
1.00	100.0	1.080	1.100	1.170	1.100
1.15	12.5	1.120	1.190	1.230	1.150
1.15	25.0	1.115	1.170	1.220	1.140
1.15	50.0	1.120	1.155	1.230	1.145
1.15	100.0	1.115	1.140	1.225	1.140

CASE 3: EFFECT OF THE FILM COEFFICIENT OF HEAT TRANSFER: FRONT-TO-BACK RATIO = 1.15; RAMP TIME = 12.5 msec

FILM COEFFICIENT OF HEAT TRANSFER	HEAT-FLUX RATIO			
Btu/hr-ft^2-^{o}F	STEADY STATE AT 100 MW	FIRST PEAK	SECOND PEAK	STEADY STATE AT 300 MW
17,400	1.125	1.180	1.220	1.140
16,800	1.120	1.190	1.230	1.150
15,600	1.120	1.180	1.260	1.140

*ALL HEAT FLUX RATIOS ARE ±0.005.

It appears from this study that the assumed hot spot factor corresponding to heat-flux ratio of 1.15 that has been used in the steady-state analysis is adequate. However, this analog computer investigation will be continued. The effect of varying physical properties and uneven channel spaces will be explored for a power transient corresponding to a $0.75 step in reactivity. The effect of the study on the hot spot factors used in the steady-state and transient analysis will then be evaluated.

A parametric, steady-state heat transfer study of the AARR has been made for the case of an axial heat-flux distribution with a max/avg of 1.5 over the last 6 in. of the fuel. The effect of inlet temperature, flow rate, and varying channel spaces was studied. The results must be analyzed in greater detail, but indications are that the best method of attaining high power levels from a heat transfer and fluid flow viewpoint will be to utilize a core that orifices or distributes the flow throughout the core. It appears that a core composed of three annular rings in which a metal-to-water (M/W) ratio of about 0.80 for the inner and outer rings and a M/W ratio of about 1.0 for the intermediate annular ring were used would greatly improve the steady-state performance of the AARR. This configuration would also provide better transient-reactivity feedback if the flow in the intermediate ring were reduced.

The effect of this type of core on the physics and transient behavior must be checked.

3. Transient Analysis

Analog studies were made for two simulated operational abnormalities, viz., (1) continuous withdrawal of a control rod and (2) injection of cold water into the reactor. The conditions considered to describe each of these problems and the results obtained from the calculations are as follows:

a. Case 1. A startup accident is simulated with the reactor assumed to be critical at essentially zero power (2.4×10^{-4} W) followed by the continuous addition of reactivity at a rate of 5×10^{-4} k_{ex} per second. This is considered to correspond to the reactivity-addition rate due to the continuous withdrawal of a control rod from a position of maximum differential worth at maximum rod speed. Since negligible reactivity compensation is developed due to inherent feedback mechanisms until reactor power reaches 1 MW, the initial portion of this problem was solved by use of the digital code RE-101 without feedback. The values of reactivity, neutron density, and delayed-neutron precursor concentrations thereby obtained for 1-MW power were used as input conditions for the analog program for continuation of the problem with feedback.

After initiation of the transient, the time to reach 1-MW power is 15.75 sec. At this point, total reactivity is 78.75×10^{-4} k_{ex}, or essentially prompt critical, and the reactor period is approximately 50 msec. Power continues to rise exponentially for an additional 140 msec to a level of approximately 12.5 MW, at which sufficient feedback reactivity is developed to reverse the exponential power rise. Net reactivity at this point is reduced to 78.08×10^{-4} k_{ex}, or slightly subprompt critical. Following this, the ensuing power rise is accompanied by sufficient feedback reactivity such that the power rises nearby linearly with time. At 100 MW, which is

reached at 17.66 sec after initiation of the transient, the power rate is approximately 40 MW/sec. Termination of this excursion before hazardous conditions develop is considered to be well within the capabilities of the AARR safety systems.

b. Case 2. The consequences of the injection of cold water into the reactor were examined by simulating the effects of instantaneous reduction in normal inlet water temperature to the freezing point. Although the physical realization of this condition is not feasible, it is considered to represent the theoretical upper limit insofar as the resulting power excursion is concerned. The transient is initiated from a simulated equilibrium reactor power level of 100 MW with full coolant flow.

The reactivity produced due to cold water injection is that resulting from the combined effects of the negative temperature coefficients in the core and the positive coefficients in the internal thermal column and beryllium reflector. In the simulation, no credit was taken for the beneficial effect of the beryllium reflector.

The net reactivity rises rapidly following reduction of inlet water temperature, reaching a maximum value of approximately $4.8 \times 10^{-3}\ k_{ex}$ at 33 msec, which is the water transit time through the core. The resulting power rise reaches a peak value of 255 MW at approximately 37 msec following initiation of the transient, and then decays to a quasi-equilibrium level of approximately 160 MW. Conditions at the hot spot remain well below critical values; the surface temperature remains below saturation and, hence, no local boiling occurs during this transient.

4. Instrumentation Control Design

The R101 code was used to check the results of the analog for step-reactivity insertions. Data from these calculations checked very closely with those of the analog computer and helped establish confidence in the work done to date.

A number of calculations were made to simulate the rod-withdrawal accident. Several reactivity insertion rates were used to bracket a rate for use in the determination of the maximum allowable speed of control rod operation. The principal reason, however, was to provide information computed from source level to power level of reactor operation for use as an input in the analog. (The analog is not capable of computing over this many decades of operation, and the existing codes do not include a satisfactory method of introducing reactivity feedback over the power range.) Complete information at the start of power operation was provided by modifying the R101 code to provide the final C_i values for use in the analog.

Some time was spent programming the LGP-30 to calculate the range of voltage and current needed in a power supply to provide electrical heating in a fuel element. All that is needed to use the code are values of heat dissipation, the electrical characteristics of the material being heated, and the temperature range of operation.

5. Critical Experiment

Foil activations, danger coefficients, and the Rossi-alpha were measured in the 615-fuel-foil core (see Progress Report for December 1964, ANL-6997, pp. 54-55). Cadmium ratio (Cd.R) measurements were made with gold, copper, dysprosium, indium, manganese, and U^{235} fission foils. The values obtained for this core indicated a substantial decrease in the quantity (Cd.R - 1), which is the ratio of subcadmium to epicadmium activation. The values of the cadmium ratio of gold and indium were so near to unity that remeasurement is planned by the dysprosium substitution method, which is more sensitive than direct measurement.

Danger coefficient measurements gave significantly reduced worth in this core than in the 315-fuel-foil core for the same samples. The change was greatest in the thermal-neutron absorbers (fuel and cadmium) and least in resonance energy neutron absorbers.

A preliminary value for water worth by Teflon displacement from the 0.1-cm-thick coolant channels was 36% greater than in the 315 fuel foil core.

Data treatment is being continued to obtain final values for the above measurements. Further work is planned including a temperature-coefficient measurement and various loading modifications preliminary to reloading with higher fuel concentration.

B. Regenerative Fuel Cells

1. Bimetallic Cells

a. Sodium-Bismuth Cell Studies. A sodium-bismuth cell (without a thermal regenerator) is being operated to define some of the engineering problems associated with cell operation. The cell, whose anode and cathode sections are 3 in. in diameter, is constructed of Type 304 stainless steel and is equipped with a frozen electrolyte-silicone rubber insulator seal. The cell was put into operation at a temperature of about 550°C with a charge of 400 g bismuth, 15.5 g sodium, and 313.6 g electrolyte (the ternary eutectic 53.2 m/o NaI-31.6 m/o NaCl-15.2 m/o NaF). Periodic regeneration was accomplished electrically by reversing the cell current.

The cell has now been operating for 45 days. The objectives of the continued operation are to determine (1) the effects of operation on the freeze seal-insulator and stainless steel cell, and (2) the effects of operation variables, such as temperature and current, on cell behavior. At present the freeze seal-insulator is functioning well, and the stainless steel cell shows no evidence of deterioration. Operation will be continued until a component failure occurs.

b. Engineering Material Study. Dynamic corrosion studies of low carbon steel by liquid bismuth and bismuth-sodium alloys were continued. The tests are being conducted to find suitable materials of construction for the sodium-bismuth regenerative cell system. An experiment in which bismuth was circulated in a thermal convection loop with a hot-leg temperature of 850°C and a cold-leg temperature of 450°C was described in the Progress Report for November 1964, ANL-6977, p. 80. Attack of the low carbon steel by bismuth caused a leak in the hot-leg section of the loop after 430 hr of operation. In a repetition of the experiment, carried out to verify the previous results, similar attack occurred and a leak developed after 279 hr of operation.

A thermal convection loop of low carbon steel containing an alloy of bismuth-20 a/o sodium was also operated under the same temperature conditions (hot-leg, 850°C; cold-leg, 450°C). After 125 hr of operation, attack of the mild steel by the bismuth-sodium alloy caused failure of the loop. The general pattern of corrosion was similar to that observed when pure bismuth was used. It is not certain whether the higher rate of corrosion was caused entirely by the addition of sodium. It is possible that impurities (such as oxygen) associated with the sodium were responsible for the increased rate of corrosion. It is certain, however, that low carbon steel is not a suitable material of construction for the high-temperature section (regenerator) of the sodium-bismuth cell. Currently, a loop made of Type 316 stainless steel and containing pure bismuth is in operation with a hot-leg temperature of 850°C and a cold-leg temperature of 450°C.

IV. NUCLEAR SAFETY

A. Chemical Reactions

1. Metal-Water Reactions

a. Scale-up Experiments in TREAT. From results of particle-size determinations on the residues from experiments CEN 196-S (see Progress Report for November 1964, ANL-6977, p. 85) and CEN 197-S (see Progress Report for December 1964, ANL-6997, pp. 57-58), calculations have been made of the changes in surface area resulting from the transients. In CEN 196-S the surface area of the fuel was increased by a factor of 2.7. In CEN 197-S the surface area after the transient was 28.7 times the original surface area of the fuel rods.

In Figure 17 is a plot of the fission energy input versus the increase in surface area for all of the metal-water experiments in TREAT with uranium and uranium-alloy fuels. All experiments except CEN 196-S and CEN 197-S were conducted with single fuel rods. It is evident from the figure that (i) there is an energy threshold (about 100 cal/g U) below which destruction of uranium fuels does not occur, and (ii) significant increases in surface area of uranium fuels can occur when the energy input is above this threshold value.

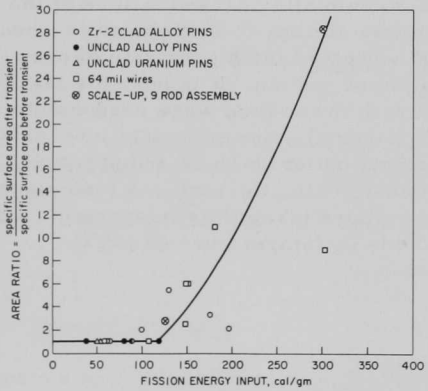

Figure 17

TREAT Uranium-Water Experiments: Change in Surface Area vs. Reactor Energy Input

Future metal-water scale-up experiments are planned in which clusters of stainless steel-clad UO_2 and Zircaloy-2-clad UO_2 fuel rods will be exposed to transients in TREAT.

b. Short-period Transient Irradiations. The metal-water experiments being carried out in connection with the Kiwi-TNT destructive test (see Progress Report for November 1964, ANL-6977, p. 86) were conducted

on Jan. 12, 1965 at the Nuclear Rocket Development Station at Jackass Flats, Nevada, as a part of the Los Alamos Rover Program. In the single, short-period (0.5-msec) excursion, the Kiwi reactor was completely destroyed. Prior to the test twenty-four autoclaves for the metal-water experiments were mounted in positions external to the reactor at various distances from the core so that fuel specimens within the autoclaves would be exposed to a range of energy inputs. Six specimens of four different fuels were used. These were Zircaloy-2-clad, UO_2-core pins; Type 304 stainless steel-clad, UO_2-core pins; uranium-5 w/o zirconium-1.5 w/o niobium alloy pins; and uranium-aluminum fuel plates of the SPERT type.

At the conclusion of the destructive test, 22 of the 24 autoclaves located at various distances from the reactor were recovered intact at distances from 30 to 500 ft from the reactor. One autoclave was ruptured; one has not been found. The recovered autoclaves are being shipped to Argonne. Determinations will be made of the extent of metal-water reactions, the burnup of the samples, and the particle-size distribution; these data will be correlated with data for the reactor excursion. The results of these experiments will then be compared with the metal-water experiments conducted in the TREAT reactor.

B. Reactor Kinetics

1. Fast Reactor Safety

a. Transients with Thorium-Uranium Fuel. Six EBR-II Mark-I-type Th-U fuel pins, previously subjected to transient nuclear heating in TREAT experiments (see Progress Report for December 1964, ANL-6997, p. 59) were examined. Each specimen consisted of a fuel cylinder of thorium-20 w/o uranium alloy, approximately 12 cm long and 0.356 cm in diameter, sodium-bonded to a steel jacket of 0.442-cm outer diameter and 0.023-cm wall. They were exposed in standard transparent meltdown capsules. Two fast-response thermocouples were spotwelded to the surface of each cladding tube. Five samples were given short nuclear power bursts of approximately 0.3-sec duration, and one was given a flattened power excursion of comparable integrated power, but ~15-sec duration.

The threshold for cladding failure was found to occur at a cladding surface temperature of approximately 1350°C, which was in reasonable agreement with a bursting pressure estimate of ~1305°C made for an isothermal sample model. Sample No. 1 had a maximum recorded cladding temperature of 1190°C and showed no signs of failure. Sample No. 2, with maximum cladding temperatures of 1315 and 1350°C reported by the two thermocouples, did not fail, but showed evidence of selective melting and flow of a molten phase which solidified against the inside surface of the cladding without penetrating. Sample No. 3, which reached about 1400°C, just above the failure threshold, showed greater fuel-cladding alloy

formation and minor fuel flow from the cladding, apparently under the influence of gravity alone (see Figure 18). Sample No. 4 (given the constant power transient) showed comparable attack on the cladding (see Figure 19). The last two pins, No. 5 and No. 6, were run to extensive failure, but also gave evidence of fuel motion dominated by gravity (see Figure 20).

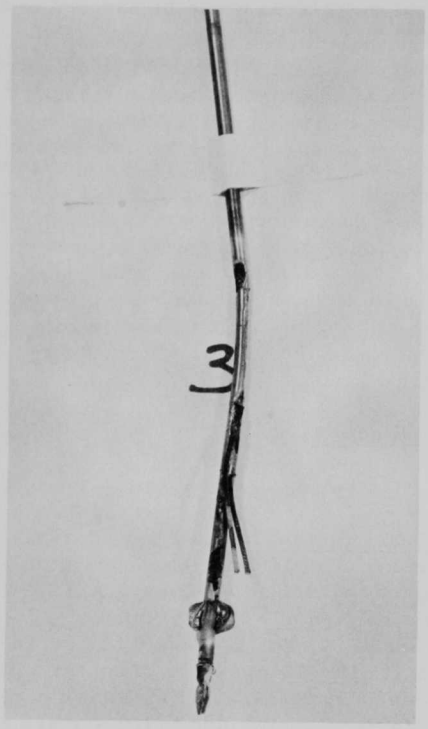

Figure 18

Appearance of Sample No. 3, Showing Dissolution of Cladding along the Fuel, a Localized Rupture of Cladding at the Bottom (Apparently due to Internal Pressure), and Drops of Material Which Had Run down the Inside of Cladding and Solidified at the Region of Rupture. Thermocouple wires are still attached.

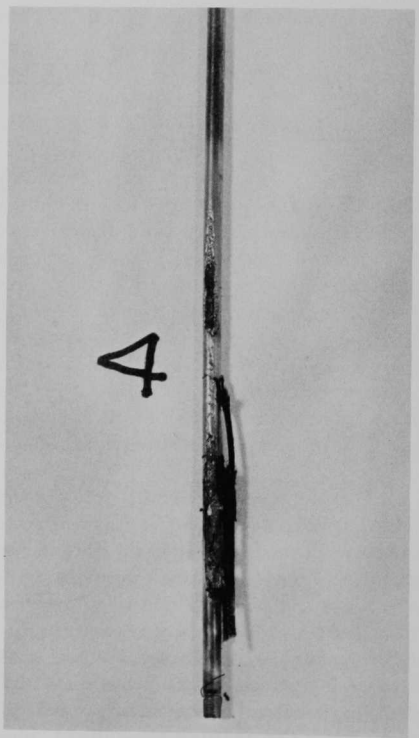

Figure 19

Appearance of Sample No. 4, Showing the Dissolution of Cladding and Formation of Fuel-cladding Alloy. Thermocouples are still attached.

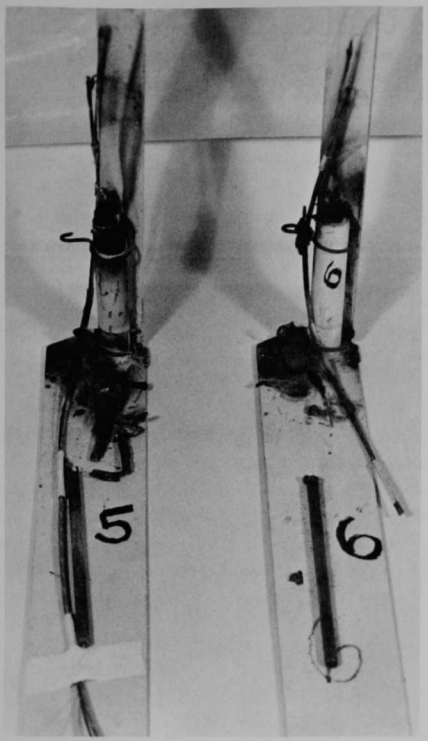

Figure 20

Appearance of Samples 5 and 6, Both of Which Suffered Extensive Failure. Although sodium was expelled vigorously from the cladding upon failure, the predominant mode of movement for the melting fuel was to fall downward due to gravity.

High-speed color motion pictures taken of the experiments showed high-velocity release of sodium from the cladding. Because the fuel remained relatively intact at the time of failure, it was not expelled vigorously by the sodium as has been found to be the case with standard EBR-II Mark-I elements, which contain fuel that melts in a range of about 1000-1080°C. The melting point of the thorium-uranium alloy tested is estimated to be 1477°C (with a liquid phase appearing at 1090°C).

This behavior might be modified significantly, however, by such conditions as greatly different heating rates, presence of sodium coolant, and effects of fission products.

Specimens have been taken for metallographic analysis in order to determine the progression of melting, the tendencies for agglomeration or movement of liquid phases, and the interaction of fuel and cladding.

2. TREAT Operations

a. Large TREAT Loop. The rework of the compound bellows assemblies for expansion joints is essentially 75% completed. Several weld joints had to be reworked.

Two shipments of single bellows components from Flexicraft Industries have been received at ANL. These shipments represent a portion of the total delivery and subject to inspection will immediately be incorporated into their respective assemblies.

The design drawings of the test section have been finished. Two sets of prints have been forwarded to Idaho for review. If these are acceptable, the prints will be prepared for bid submission.

The Owens Corning Company indicates that the boron content of the Kaylo insulation to be used in the test section is less than 0.01%, which will allow use of the insulation for the purpose intended.

Prints of the complete gas system together with bills of material have been checked and are now being reviewed by the operating staff.

Price and delivery information have been obtained for the remaining unordered gas-system components. Quotations for two bellows-sealed, pneumatic-actuated valves, to be used as shutoff valves in the gas lines to the dump and the storage vessels, indicated they would not meet a seat leakage rate of 10^{-6} cc He(at STP)/sec, but that the leakage rate would be much higher. These valves would be unsatisfactory if tight shutoff is required.

As an alternative, the "McCannaseal" ball valve equipped with a Graphitar seat is suitable for operation at conditions up to 75 psi and 1000°F. Although this valve will not meet the above seat leakage rate, it is expected that its seat leakage rate will be lower than that of the pneumatic-actuated, bellows-sealed valve. If a small seal leakage rate can be tolerated, it is proposed to replace the packless, bellows-sealed valve with Graphitar-sealed ball valves.

V. PUBLICATIONS

Papers

PROCESSING OF FUEL MATERIALS BY PYROMETALLURGICAL METHODS
S. Lawroski and L. Burris
Atomic Energy Review 2(3), 3 (Nov 1964)

COMPOUNDS OF INTEREST, REPORT ON INTERNATIONAL SYMPOSIUM ON COMPOUNDS OF INTEREST IN NUCLEAR TECHNOLOGY, UNIVERSITY OF COLORADO, BOULDER, AUGUST 3-5, 1964
M. Tetenbaum
Nucl. News 7(12), 24-28 (Dec 1964)

CALORIMETRY
W. N. Hubbard
Science 147, 312-314 (Jan 15, 1965)

COMPARISON OF NEUTRON EMBRITTLEMENT OF STEEL IN DIFFERENT REACTOR SPECTRA
A. D. Rossin
Nucl. Structural Engr. 1(1), 76-82 (1965)

INFLUENCE OF INTERNAL THERMAL RADIATION ON HEAT TRANSFER IN UO_2 FUEL ELEMENTS
Raymond Viskanta
Nucl. Sci. Eng. 21, 13-19 (Jan 1965)

MODERATOR SCATTERING AND FLUX DEPRESSION NEAR RESONANCES
P. F. Gast
Nucl. Sci. Eng. 21, 191 (Jan 1965) Letter

ANL Reports

ANL-6778 STRUCTURAL ANALYSIS OF FARET CORE SUPPORTS UNDER MECHANICAL AND THERMAL LOADINGS
M. M. Chen

ANL-6828 PRELIMINARY PHYSICS AND HEAT TRANSFER DESIGN CALCULATIONS FOR A ROCKET FUEL TEST REACTOR (RFTR)
D. R. MacFarlane and J. T. Madell

ANL-6900 CHEMICAL ENGINEERING DIVISION SEMIANNUAL REPORT, January-June, 1964

ANL-6915 FLUX TRAP EXPERIMENTS IN D_2O-MODERATED THORIA-URANIA CORES
K. E. Plumlee

ANL-6926 THEORETICAL STUDY ON THE TRANSFER FUNCTION OF BORAX-V WITH CENTRAL SUPERHEATER
Jiro Wakabayashi

ANL-6927 A ZONED LOADING FOR A ZPR-III-TYPE FACILITY
A. G. Edwards

ANL-6934 INTERBUILDING FUEL TRANSFER COFFIN FOR THE EBR-II REACTOR
G. J. Bernstein, A. A. Chilenskas, and R. F. Malecha

ANL-6935 SOME CONSIDERATIONS ON THE MELTDOWN PROBLEM FOR FARET
P. J. Persiani, A. Watanabe, U. Wolff, S. Grifoni, and B. Warman

ANL-6966 DESIGN OF A REMOTELY REMOVABLE AND REPLACEABLE CRANE-BRIDGE DRIVE UNIT FOR THE EBR-II FUEL CYCLE FACILITY
Johan E. A. Graae

B